Contents lists available at SCCE

Journal of Soft Computing in Civil Engineering

Journal homepage: www.jsoftcivil.com

Predictive Models for Prediction of Broad Crested Gabion Weir Aeration Performance

Nand Kumar Tiwari[1*], KM Luxmi[2], Subodh Ranjan[3]

1. Associate Professor, Department of Civil Engineering, National Institute of Technology, Kurukshetra (Haryana), India
2. Ph.D. Scholar, Department of Civil Engineering, National Institute of Technology, Kurukshetra (Haryana), India
3. Professor, Department of Civil Engineering, National Institute of Technology, Kurukshetra (Haryana), India
*Corresponding author: *nand@nitkkr.ac.in*

https://doi.org/10.22115/SCCE.2023.357761.1516

ARTICLE INFO

Article history:
Received: 26 August 2022
Revised: 19 December 2022
Accepted: 31 January 2023

Keywords:
Gabion weir aeration-performance efficiency;
Neural network;
Neuro-fuzzy;
Deep neural network;
Empirical relations;
Sensitivity performance.

ABSTRACT

The gabion weirs serve the same functions that their counterpart impervious weirs do. However, they have the advantage of being eco-friendly, more stable, and economical in low to medium-head cases. Dissolved oxygen is one of the major determinants for the assessment of the purity of water. The purpose of the present work is to illustrate the comparison of multiple linear regression (MLR), neural network (NN), neuro-fuzzy system (NFS), deep neural network (DNN), and reported empirical models for the prediction of gabion weir aeration performance efficiency (APE_{20}) with experimental results which are collected from the laboratory test. The NFS with four shaped membership functions, NN, DNN, MLR, and existing empirical models, are generated with the same input parameters, and their potentials are assessed to statistical appraisal indices. The results show that the DNN with the highest value of R^2 (0.935) and NSE (0.934) and having the least errors in validating phase is the outperforming proposed model in the prediction of the $APE_{20,}$ which the NN model follows with R^2 (0.917) and NSE (0.917). However, except trapezoidal shaped NFS model with R^2 (0.873) and NSE (0.852) and MLR with R^2 (0.905) and NSE (0.897), the remaining models of NFS-based and empirical relations could not perform better in validating phase. The sensitivity performance test is too conducted to find the relative relevance of the input parameter on the results of the APE_{20}, where discharge per unit width (q) is found to be the most significant parameter, followed by the drop height (H_0).

How to cite this article: Tiwari NK, Luxmi KM, Ranjan S. Predictive models for prediction of broad crested gabion weir aeration performance. J Soft Comput Civ Eng 2023;7(2):43–73. https://doi.org/10.22115/scce.2023.357761.1516

1. Introduction

Gabion weirs are the fluidic devices used in retaining and diverting water and for discharge measurement by maintaining the hygienic environment and ecological balance in the river system because silts and organic materials can go downstream through their pervious body, help in the minimization of siltation in the upstream. Besides, bacteria living between the gabion particles also help decompose organic materials.

The dissolved oxygen (D.O.) level in water for a river life system has been a significant parameter for assessing water quality. The D.O. level in water is often higher in rural streams because these streams get fewer impurities compared to urban streams. In case the D.O. level in urban rivers, ponds, lagoons, etc., rises, aerobic activities are encouraged, improving the condition of local aquatic lives. Therefore, rejuvenating the river ecosystems is significant work [1]. Oxygen solubility in water depends on impurity, temperature, and pressure, as impure water has lesser oxygen than healthy water. Oxygen from the atmosphere dissolves in the water bodies. Water takes oxygen when streams and rivers pass through rocks. Activities like aeration, photosynthesis and many more constantly change the D.O. levels.

The quality of surface water should include recent technical results about contamination and its consequence on individual conditions and water life. Surface waters are utilized for multi-purposes, including water supplies, navigation, power generation, fishing cultures, and many more. In case of a fall of D.O. level in the water, even below the normal level of 4 ppm, the maintenance can be made out with fluidic devices like Parshall flumes, spillways, and weirs. Ecological standard properties for water surfaces differ depending upon their uses and from country to country. Therefore, the D.O. level is an essential determinant for the general quality measurement of river/canal water. Gabion weirs, spillways, and other hydraulic structures can enhance the D.O. level by creating vortexes, jumps, and trapping air from the atmosphere into the water. Aeration is usually utilized to enhance the D.O. level in water bodies [2]. In energy dissipation under sluice gate and other fluidic devices, the air is too trapped in the water flow. Therefore, natural aeration occurs, and the D.O. level in water is subsequently enhanced. Since water passes over hydraulic structures, water sucks oxygen from the air. This development has ecological effects on waterways and hydraulic devices, for instance, the water life may come under strain when the D.O. level is dipped below a certain level, and water may have an offensive smell. Numerous analyses have studied the standard concentration for water quality concerning D.O. levels. A broad variation of D.O. levels decides normal concentrations for water quality. Current findings [3–7] suggest the concentration of oxygen transfer efficiency of fluidic devices required to keep up and increase water quality. Chu et al. [1] detailed that oxygen transfer through fluidic devices is an environmental-friendly, optimal technique for correcting D.O. concentration in contaminated water bodies.

Fluidic devices significantly impact dissolved oxygen concentration levels in water bodies, even when the water just touches the fluidic device for a short period. The oxygen aeration efficacy of

fluidic devices has been examined by various investigators [1,8–13], and many investigators [8,9] have specified that hydraulic structures cannot only be utilized as energy dissipators but also be used efficiently for the natural aeration of the river system. Many works have been carried out on effectively utilizing fluidic devices in oxygen aeration transfer [8–15]. A cascade is effective in surface water aeration in events of enough drop height. Various weirs can be utilized for aeration purposes, and in these circumstances, the aeration process has been effective and economical as it does not require any energy. Several pressure arrangements like venturi and conduit devices are used for surface water oxygenation, but in these cases, oxygenation would incur money due to the energy needed for their operations.

Nowadays, soft computing techniques have wide applications in the discipline and domain of engineering. Tiwari and Sihag [12] studied the potential performance of ANN, FL, and ANFIS in predicting the aeration of the Parshall flume. Kumar et al. [16] investigated the effect of jet parameters in the aeration of water in the tank and the oxygen transfer coefficient (Kla). An empirical relation has been derived. Besides ANN, GRNN, MARS, and ANFIS are utilized to estimate the oxygen transfer coefficient. Kumar et al. [17] utilized kernel functions to predict the Kla for a hollow jet. Modeling tools ANN and empirical equations are used by Kumar et al. [17] in estimating the Kla of pressure water jets. Aeration study and modeling methods are used to predict oxygen transfer of hollow jet aerators by Kumar et al. [18]. Bandana et al. [19] investigated soft computing tools in predicting penetration depth for hollow jets. Sattar et al. [20] studied the stepped weir and estimated its aeration efficiency with A.I. models. Gerger et al. [2] applied machine learning models to assess water's oxygenation at chutes. Sharafati et al. [21] evaluated the performance of sediment ejectors with integrated ANFIS models. Gameson [22], Markovsky and Kobus [23], and Nakasone [24] added more in the field of oxygen transfer at hydraulic devices. Some more significant parameters, like penetration depth by bubbles, residence time, drop height, fall velocity, etc., also affect the aeration process [25,26]. Preul and Holler [27] studied oxygen transfer at the low dam, while Markofsky and Kobus [23] discussed the re-oxygenation aspect at the weir. However, Nakasone [24] worked on oxygen transfer at both fluidic devices of cascade and weir, but Watson et al. [28] made a study for aeration assessment of the low drop weir. Luxmi et al. [29], using test data sets for the assessment indicators of RMSE and CC, compare the accuracy of the neuro-fuzzy, neural network, and Gaussian process regression models in estimating the gabion weir oxygen aeration efficiency. A developed model has been used to study the aeration performance of the Montana Flume [30] and the prediction of Adaptive Neuro-Fuzzy Inference System (ANFIS), Multilinear Regression (MLR), and Multi Non-linear Regression (MNLR). Tiwari et al. [31] applied multi-non-linear regression (MNLR), adaptive neuro-fuzzy inference system (ANFIS), and artificial neural network (ANN) models in the estimation of Montana flume aeration. The aeration efficiency of stepped gabion weirs is computed using Random Forest (RF) and Artificial Neural Network (ANN). By conducting experiments in a laboratory flume and input parameters such as mean size, porosity, discharge, and drop height, the actual aeration efficiency is determined [32]. The current paper [33] examines the performance of the application of three soft computing

techniques, including the deep neural network (DNN), backpropagation neural network (BPNN), and adaptive neuro-fuzzy inference system (ANFIS), to forecast the gabion spillways' oxygen aeration efficiency (OAE20). In addition, past studies and conventional equations were used to predict OAE20 of the gabion spillways, including multivariate linear and nonlinear regressions (MVLR and MVNLR).

In order to frame the correlations for predicting the values of volumetric oxygen transfer coefficient (KLa) experimental test data from a variety of configurations of plunging hollow jet aerators are investigated, with the jet variables (discharge, jet thickness, jet velocity, jet length, depth of water pool, pipe outlet diameter, number of jets). The neuro-fuzzy (ANFIS), support vector regression (SVM), artificial neural network (ANN), M5 tree (M5), and random forests (RF) approaches are compared with the nonlinear regression modeling equations obtained from dimensional and nondimensional data sets [34]. The machine learning techniques [35] were used to estimate the oxygen aeration performance efficiency (OAPE20) of the gabion spillway by using the gradient boosting machine (GBM), neural network (NN), and deep neural network (DNN). Along with the previous models, conventional equations developed by multivariable linear regression (MLR) and multivariable nonlinear regression (MNLR) are also used to estimate the OAPE20 of the gabion spillways.

The data mining algorithms [36], backpropagation neural network (BPNN), adaptive neuro-fuzzy inference system (ANFIS), and multi-variant linear and nonlinear regression (MVLR and MVNLR) are developed with experimental data to estimate the gabion oxygen transfer efficiency and their results are compared. The potential for estimating aeration efficiency (E20) at labyrinth weirs using the M5P model tree (M5P), support vector regression machine (SVM), and random forest (RF) methods [37]. Evolutionary polynomial regression models [38] developed with an exponential function were selected as the optimal models. According to the R^2 coefficient, the levels of precision of the model in predicting collapse settlement using training, testing, and all data were 0.9759, 0.9759, and 0.9759, respectively, and the precision levels in predicting the coefficient of stress release are 0.9833, 0.9820, and 0.9833, respectively. The purpose of the study [39] is to develop and assess machine learning-based prediction models for estimating the dynamic modulus of hot mix asphalt using ANNs, GP, and the Combinatorial Group Method of Data Handling (GMDH-Combi).

1.1 Aeration at fluidic structures

Fluidic structures can generate cross-flow, resulting in tiny bubbles that are moved up to the whole flow and, consequently, a surge in D.O. concentration. In a solitary fluidic device, oxygenation equivalent to the volume that would take place over many miles in the water bodies could be noticed because such a device is highly cross-current, producing an enhanced interfacial rejuvenation.

Weir is constructed to operate the water supply, discharge measurement, or divert the water. Water plunging over and through the weir pulls and sucks air as it drops into the water pool. Exceptional contributions to the aeration efficiency of hydraulic devices are made by Gameson [22], Markovsky and Kobus [23], and Nakasone [24]. Trilateral weirs perform better than rectangular weirs, but among the trilateral weirs, multiple triangular weirs give better results than single weirs. Drop height, roughness, and fall velocity are important parameters that affect the aeration besides residence time, and air bubbles' penetration depth also controls the aeration process [25,26].

1.2. Significance, objective, and novelty

Gabion weir provides an alternate design that can be utilized for river training, flash flood control, and rapid dissipation of energy. It is also used to slow down the runoff velocity and stabilize slopes.

There are many aspects to the novelty and objective of the current study.; the literature review indicates a recognition that no prior work has been identified with the machine learning (ML) methods to predict gabion weir aeration performance efficiency (APE_{20}) that too by applying neural network (NN), neuro-fuzzy system (NFS), deep neural network (DNN) and multiple linear regression (MLR) to identify and fill the gap-grey area by generating and verifying algorithms for the APE_{20} of the gabion weir. Initially, the estimation of the APE20 of the gabion weir is outlined in the present study by performing the laboratory test by varying gabion weir height, gabion material mean particle size, gabion weir length, plunging drop height, and discharge per unit width of the gabion weir. Secondly, the APE_{20} of the gabion weir is developed, computed, and compared with proposed soft computing algorithms employing experimental data. The prediction ability of the models is evaluated in respect of performance metrics. Additionally, the predicted results of the APE_{20} of the gabion weir through NFS, NN, DNN, MLR, and existing proposed mathematical models are compared amongst themselves to have the best-performing model. Finally, sensitivity investigation was used to determine the comparative relevance of input variables on the APE_{20} results of the gabion weir.

1.3. The basic definition of aeration efficiency

The aeration performance efficiency (APE) is described below:

$$\text{APE}= 1 - \frac{1}{\text{DR}} = \frac{I_{dstream} - I_{ustream}}{I_{Saturated} - I_{dstream}}$$

$$\text{Where, DR= Deficit Ratio} = \frac{I_{Saturated} - I_{ustream}}{I_{Saturated} - I_{dstream}}$$

$I_{dstream}$ and $I_{ustream}$ stand for downstream and upstream intensity of the D.O., respectively, and aeration performance efficiency, APE, for any water temperature. Usually, the temperature correction factor is calculated by the equation given below

$$1 - \mathrm{APE}_{20} = 1 - \mathrm{APE}^{1/\left(1.0+0.02103(\mathrm{Temprature}-20)+8.261\mathrm{x}10^{-5}(\mathrm{Temperature}-20)^2\right)}$$

In which, APE_{20} is the aeration performance efficiency at 20°C.

1.4. Proposed mathematical and empirical models

The aeration performance efficiency of the gabion weir depends on numerous vital characteristics that trigger the aeration process. The aeration performance efficiency (APE_{20}) equations of the traditional weir are accessible in the text, and the comparison can be made with the current analysis, and causes may be attributed that primarily both act on the concept of turbulent productions, which brings about water to suck atmospheric air. Therefore, traditional mathematical equations are evaluated in the present study, and a comparison is made with the dataset. The estimation potential of these available mathematical equations in the literature is further compared with NN, NFS, DNN, and MLR models. For the mathematical equations available in the literature, the current work can be utilized to evaluate the ability of these equations and which are enlisted in Table 1.

Table 1
Brief details of the proposed mathematical relations.

No.	Researcher	Empirical mathematical relations	Observations
1	Preul and Holler [29]	$\mathrm{APE}_{20}=1-\frac{1}{1+666\mathrm{F_r}^{-3.33}}$	Oxygenation at the low dam
2	Markofsky and Kobus [30]	$\mathrm{APE}_{20}=1-\left[\frac{1}{1+0.1\mathrm{F_r}^{1.2}}\right]^{1.115}$	Re-oxygenation study at the weir
3	Nakasone [31]	$\mathrm{APE}_{20}=1\text{-}\mathrm{e}^{(-0.0785\mathrm{H_0}^{1.31}\mathrm{q}^{0.428}\mathrm{h_w}^{0.310})}$	Aeration at weirs and cascades
4	Watson et al. [32]	$\mathrm{APE}_{20}=1-\left[\frac{1}{1+0.001\ \mathrm{F_r^2R_e^{0.32}}\left(\frac{\mathrm{h_w}}{\mathrm{H_0}}\right)^{0.7}}\right]$	Aeration assessment of the low drop weir
5	MLR	$APE_{20}=0.022q+0.003P+0.0043\ d_{50}-0.0012n+0.0018H_o-0.116$	Present study

Where, H_o=Drop height, h_w is upstream head over the crest, q is discharge per unit width, F_r is Froude number, d_{50} is the mean size of gabion particles, n is the porosity, P is the height of the gabion weir, and R_e is Reynolds number.

2. Materials and methods

2.1. Experimentation and methodology

A tilting flume experimental setup was located in the water resources laboratory of the National Institute of Technology, Kurukshetra (Haryana), India. The tilting channel measured 4.0 m, 0.25

m, and 0.3 m in length, breadth, and depth, respectively. As seen in Figure 1, the flume's sidewalls were made of transparent, ten-millimeter-thick acrylic plexiglass, and the bottom side was made of ten-millimeter-thick steel iron that was supported by a jack. The highest capacity centrifugal pump used to transfer water from the aeration tank/receiving tank to the flume has a capacity of 6 l/s. The closed re-circulating system was used to ensure that aeration of the water occurred only during the drop. The test gabion weir, which was installed at the end of the channel, water flow passed through or over the test gabion weir. The flow depth and flow volume rate of water in the flume were measured using an electromagnetic digital pointer gauge and a digital flow metre. For each reading, the receiving pool's water depth is maintained at a level that is greater than or no less than 80% of the drop height [25]. The D.O. was measured using the azide modification method.

For evaluating the quantity of aeration performance efficiency (APE_{20}) of water in the aeration tank for a particular gabion weir, the tank was filled with a fixed amount of supply water. The D.O. potential of the water in the tank was reduced to approximately 1.5 mg/l [10,11] by mixing a measured amount of Na2SO3 with CoCl2, and some water was taken from various levels of the water tank to calculate the initial D.O. intensity (Iupst). Subsequently, the experimental test was commenced for a recognized period. The test device was run for a specific period of time so that the aeration tank water D.O. level should be below the maximum saturation intensity (Isaturated) at the experiment temperature, ToC. The final dissolved oxygen intensity (Idownst) was then calculated using the azide modification technique. Using a thermometer, the water temperature in the aeration tank was recorded during the test. The method was repeated for numerous runs for tests by using three traditional weirs and twelve gabion weirs. The value of APE_{20} was then estimated. The test gabion weir was characterized by 15 exchangeable weirs (shown in Table 2) with varying flow rates, sizes of gabion particles, porosity, the height of weirs as well as drop height, and 195 data patterns of gabion weir oxygen performance efficiency were taken, and some of the readings were to cross-check the credentials of the patterns, some observations have also been made more than once.

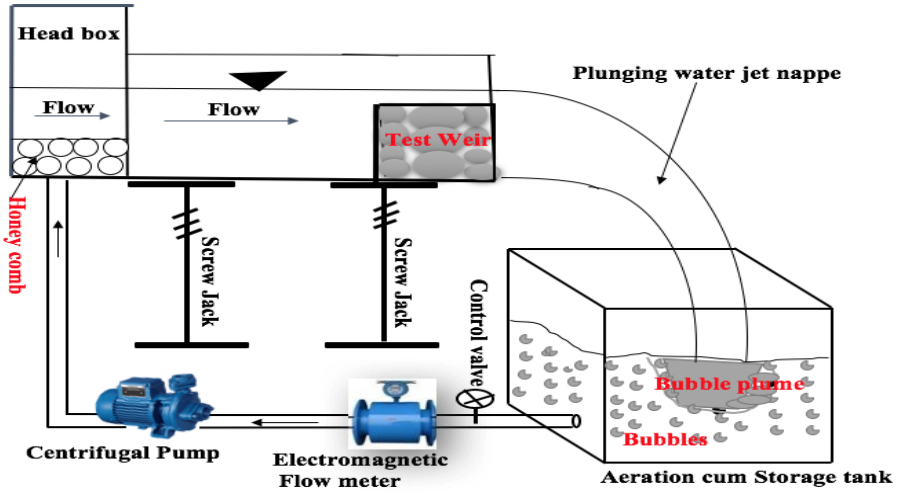

Fig. 1. Schematized view of the test setup.

Table 2
Model configuration.

Parameter	Symbol	Value	Range		Units
			From	To	
Weir height	P	10,15,20	10	20	cm
Weir length	L	60	60	60	cm
Weir width	B	25	25	25	cm
Gabion particle mean size	d_{50}	00, 10, 22.4, 31.5, 53	00	53	mm
Porosity	n	00, 35.63, 37.31, 38.43, 38.52 00, 41.99, 44.5, 46.21, 44.92 00, 43.28, 44.82, 43.73, 45.9	00	45.90	%

2.2 Framework of proposed soft computing techniques

This section presents descriptions of the conventional neuro-fuzzy system (NFS) technique. Next is the neural network (NN) technique, followed by a deep neural network (DNN).

2.2.1. Neuro-Fuzzy System (NFS)

The NFS is a soft and intelligent algorithm that utilizes and integrates an artificial neural network (ANN) learning ability with a fuzzy interference system (FIS) reasoning capability. So the power to unite the linguistic potential of the FIS with the numerical ability of an ANN, the NFS, has been proven to be a potent tool in estimating many advanced engineering processes. It was first coined by Jang [40]. The NFS has fast learning capacity and is frequently applied in classification and regression problems. It has the benefit of permitting the fuzzy rules extraction from the numeric dataset and flexibly creates a rules base. Besides, it can modify the complex adaptation of human intellect to fuzzy rules. Sugeno-type FIS, which is more prevalent, is utilized in the study. Here, modeling of training data is used by combining gradient search with least square methods. The rules are obtained by subtractive clustering of data. The input parameter is related to the output by a membership function. Practically, numerous membership functions (M.F.s) are utilized together with trapezoidal-shaped, triangular-shaped, Gaussian-shaped, etc.
Let the fuzzy inference system has two inputs, ‘s’ and ‘t,' and one output, 'f_n' a first-order Sugeno type fuzzy has the following rules:

Procedure I: if μ(s) is A1 and μ(t) is B1
then $f_{ni}= p_i\, s+ q_i\, t+ r_i$ (1)
Procedure II: if μ(s) is A2 and μ(t) is B2
then $f_{nii}= p_{ii}\, s+ q_{ii}\, t+ r_{ii}$ (2)
A1, B1, A2, and B2 are M.F.s for s and t inputs.
The general view of 5-layered ANFIS with two input variables is presented in Figure.3(a).

2.2.2. Neural Network (NN)

The NN consists of artificial neurons which are hypothetically inspired by biological nervous systems. A neural network is a regression and classification model with neurons in each layer similar to be arranged neurons in the brain, and it can learn from data patterns. It is a famous soft computing technique widely applied to water resources problems. The neurons are assigned weight and bias, which get adjusted during training. These weights and biases represent the strength of neurons. The network consists of input having nodes equal to the number of input variables, one or more hidden layers where processing takes place, and an output layer. The input is multiplied by a weight (w), and all the weighted inputs are added together with a bias (b). The sum is pushed through an activation function, and output is obtained. Many activation functions are available, like log-sigmoid, tan-sigmoid, linear, et cetera. The network trains the data fed as input using training functions like Levenberg-Marquardt (trainlm), Bayesian regularization, BFGS Quasi-newton (trainbfg), et cetera. The gradient descent algorithm is also used there to optimize the input parameter. It performs computation backward (backpropagation) and updates weight and biases where the performance function changes rapidly to achieve the target value. The transfer functions used in the present study are the log-sigmoid transfer function (logsig) activation function: Output is calculated for a given input to that layer, and generated output lies between 0 and 1. This function is mainly used in multilayer networks.

In contrast, the hyperbolic tangent sigmoid transfer function (tansig) is a good choice where the shape of the function is not essential and only speed matters and is applied for pattern recognition problems. It is a neural transfer function and is used to calculate the output of a layer from net input to that layer, and output is generated between -1 and 1. The linear transfer function (purelin) is a neural transfer function that converts net input to the output for a layer. This function is mostly used in fitting problems having output between -1 and 1. Figure 2(b) shows a general view of the three-layered neural network architecture.

2.2.3. Deep neural network (DNN)

A deep neural network (DNN) is an advanced artificial network that has transformed industrial scenarios, day-to-day lives, and several engineering disciplines in the past few years. However, its implementation in civil engineering is gradual. A DNN is a typical neural network (NN) plus depth. The depth of an NN is either measured by the presence of a massive number of nodes in the hidden layer (H.L.), decided by the number of H.L.s, or marked by hidden layers with a large number of nodes. But no threshold and single yardstick can say when NN can be recognized as deep. Conventional NN has two popular recognized nonlinear activation functions; sigmoid and hyperbolic tangent. These activation functions enable NN to learn the complexity present in the dataset. But two limitations of saturation and sensitivity [41,42] lie with sigmoid and hyperbolic tangent activation functions.

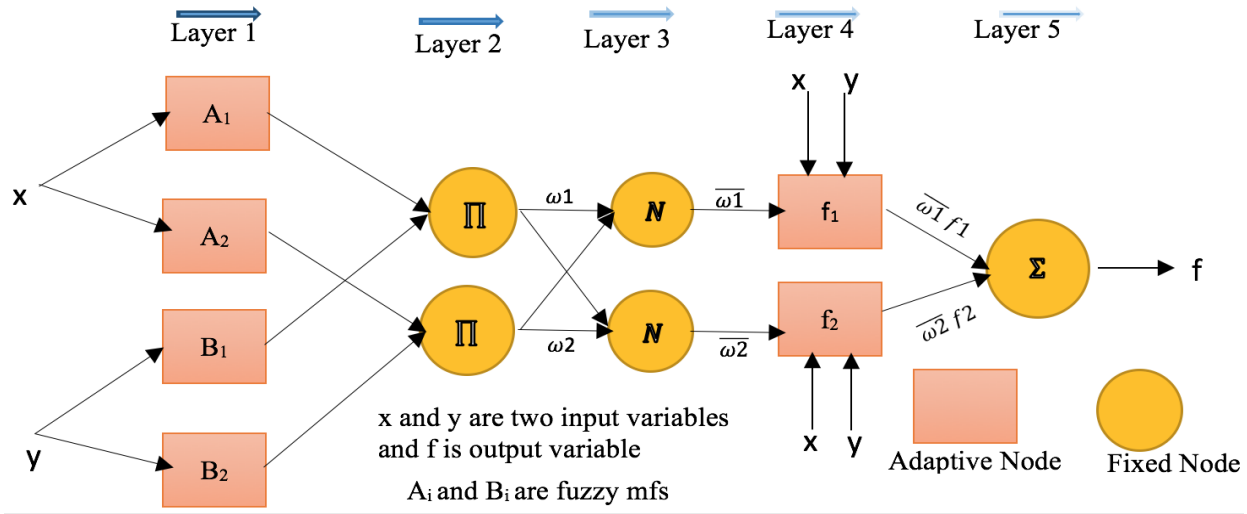

a. NFS structure

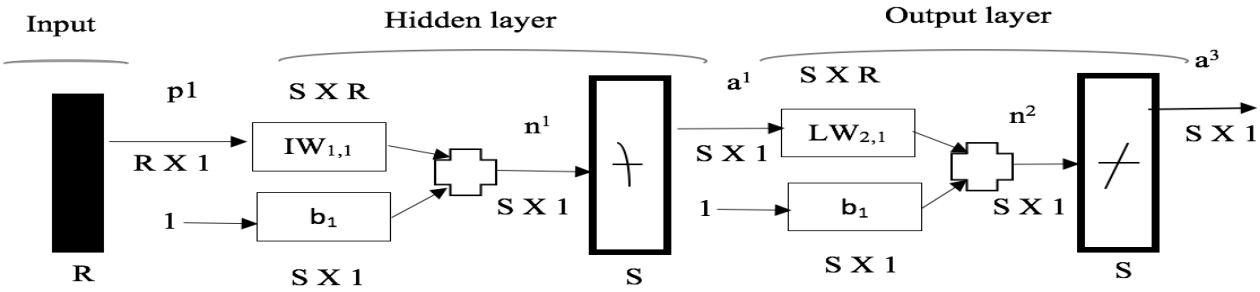

b. NN structure

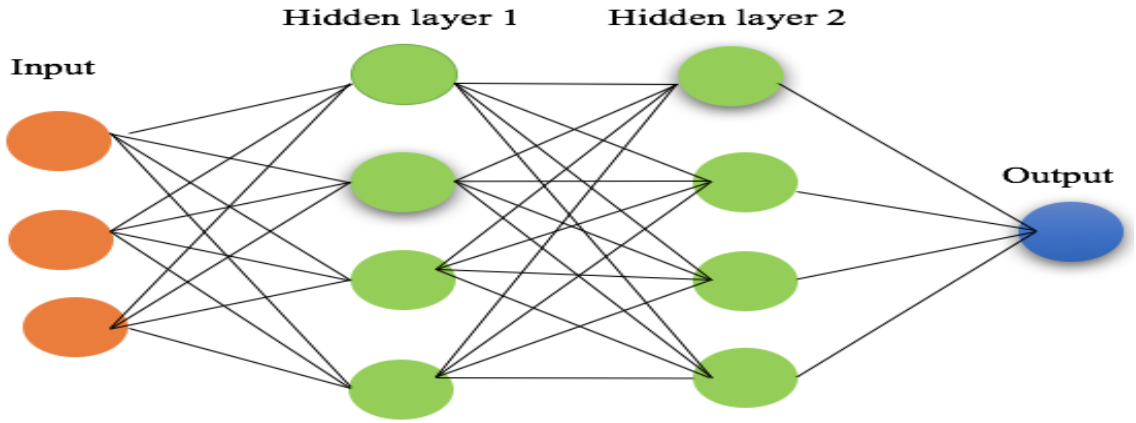

c. DNN structure

Fig. 2. Generalized structural views of (a) NFS and (b) NN (c) DNN.

The RELU (rectified linear activation) function is the piecewise collinear function and has brought a substantial algorithmic variation over the last ten years in the device of the DNN [43].

The RELU function is the most accepted function utilized in the DL, which itself outputs the

input value when it is found to be positive; otherwise, the output could be zero by default. Very easy to train and gives improved performing potential compared to alternate activation functions when applied with the DNN. The RELU function is described by $F(N_k) = Max(0, N_K)$. With a limited training dataset, the DNN may result in overfitting, consequently generating low performance in testing. To control the overfitting problem, various regularization techniques are utilized to increase the DNN model operation [41]. Regularization methods make minor changes in the learning steps to aid the model in generalization. To overcome the overfitting problem, a dropout layer introduction concept for the design of DNN was proposed by [42] to improve their generalization potential. A regularization technique, dropout, is also utilized for improving the DNN model working by pulling out a node arbitrarily, either from a hidden or visible layer, along with incoming /outgoing networks. This is attained by arbitrarily putting the neurons' weights to nil [43]. Figure 2(c) shows a general view of two hidden layered deep neural network architectures. The flow chart of predictive modeling is shown in Figure 3.

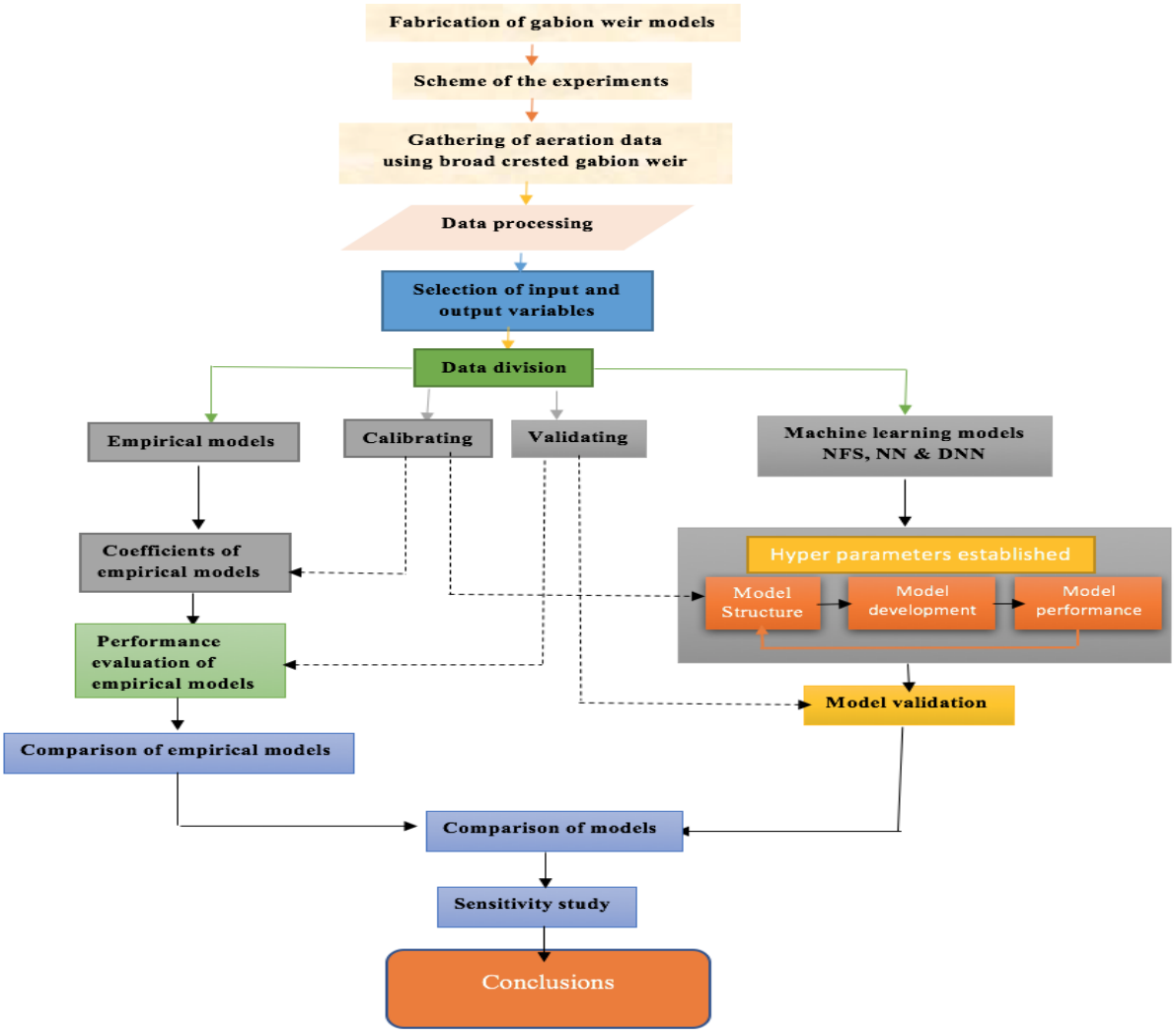

Fig. 3. Flow chart of predictive modeling.

3. Results and discussion

3.1. Model Evaluator metrics

The coefficient of determination (R2), Nash-Sutcliffe model efficiency coefficient (NSE), mean absolute error (MAE), and root mean square error (RMSE) values are computed using calibration and validation datasets to test the potential of various applied modeling skills in predicting the gabion weir aeration performance efficiency.

$$CC = \frac{n\sum_{i=1}^{n} APE20_{act}APE20_{prd} - (\sum_{i=1}^{n} AE20_{act})(\sum_{i=1}^{n} APE20_{prd})}{\sqrt{n(\sum_{i=1}^{n} APE20_{act}{}^{2}) - (\sum_{i=1}^{n} APE20_{prd})^{2}}\sqrt{n(\sum_{i=1}^{n} APE20_{prd}{}^{2}) - (\sum_{i=1}^{n} APE20_{prd})^{2}}}$$

NSE= $1 - \frac{\sum_{i=1}^{n}(APE20_{act} - APE20_{prd})^2}{\sum_{i=1}^{n}{}_{(}\, APE20_{act} - \overline{APE20}_{act})^2}$, R^2 is the coefficient of determination which is the square of a correlation coefficient, CC. The root mean square error (RMSE) and mean absolute error is defined below.

$$RMSE = \sqrt{\frac{1}{n}\sum_{i=1}^{n}(APE20_{act} - APE20_{prd})^2} \quad \text{and} \quad MAE = \frac{1}{n}\sum_{i=1}^{n} |APE20_{prd} - APE20_{act}|$$

In which $APE20_{act}$ = Actual APE_{20} values, $APE20_{prd}$ = Predictated APE_{20} values, $\overline{APE\ 20_{act}}$ = Average of actual values, and n = number of experimental patterns.

3.2. Description of aeration database

In the present study, datasets are collected from conducting laboratory tests. To generate the models, a total of 195 laboratory patterns are bifurcated randomly into two groups; 72 % of patterns (141-pattern) are selected as calibration patterns for the training of proposed models, while the remainder patterns, 28 % (54-pattern) are kept invisible to the machine learning /empirical models during models' generation process for a validation purpose (testing). The collected patterns include discharge per unit width (q), the height of the weir (P), mean gabion particle size (d_{50}), porosity (n), and drop height (H_o) as input. At the same time, aeration performance efficiency (APE_{20}) is taken as output. The summary statistical details of the pattern are enlisted in Table 3.

Table 3
Summary statistical details of calibration and validation patterns .

Variable	Units	Training			Testing		
		Range	Mean	STDV	Range	Mean	STDV
APE_{20}	-	0.013-0.611	0.321	0.1498	0.039-0.593	0.326	0.137
q	l/s/m	3.20-20.40	14.3	5.9099	3.2-20.4	14.53	0.844
P	cm	10.0-20.0	14.96	4.1049	10-20	15.08	4.099
d_{50}	mm	0-5.3	2.34	1.8288	0-5.3	2.33	1.856
n	%	0-46.21	33.76	17.1526	0-46.21	33.17	17.373
H_o	cm	46.25-76.08	33.76	7.4751	44.71-75.08	64.74	5.964

3.3. Specifications of NFS, NN, and DNN

Effective application of NFS, NN, and DNN needs optimal tuning parameters, performed by numerous trial and error steps on the calibrated and corresponding validated datasets to achieve desired outputs. The accuracy of each trial cycle is assessed in terms of four statistical performance indices, R^2, NSE, MAE, and RMSE. A smaller value of RMSE and MAE reflects a better estimation of results by the proposed models. In contrast, a more significant value of R^2 and NSE implies a stronger relationship with an experimental dataset for the proposed model predictions. The optimized values of user-defined tuning parameters are shown in Table 4.

Table 4
Optimal specifications of (a) NFS, (b) NN, and (c) DNN.

(a) NFS input mf number	Input M.F. shape	F.S.	Optimization	Output mf type	Epochs
3-3-3-6-2	Tri, Trap, Gbell, Gauss	Sugeno	hybrid	Linear/constant	3
(b) NN - topology	Training algorithm	The hidden layer transfer function	Output activation function		Epochs
5- 8 -1	trainlm	logsig	tansig		2000
(c) DNN-topology	Dropout ratio	epsilon	Output activation function	rho	Epochs
5- 2X20-1	Input =0.05; hidden=0.2	$1e^{-9}$	ReLU	0.95	8241

3.4. Results of NFS

The current work employs a neuro-fuzzy system (NFS) to model relations amongst inputs and output datasets. A Sugeno method is adopted for preparing the model. No, fixed rules exist for creating NFS models [44]. Four shaped membership functions (M.F.s), i.e., the function of triangular membership (TRIAN), the function of trapezoidal membership (TRAPZ), a combination of two gaussian membership functions (GAUS2MF), and Gaussian bell membership function (GAUS BELL) are utilized for input in NFS model. A hybrid learning process is used to train the NFS model, and each epoch combines a forward and a backward pass in the NFS training system. In the forward pass, a calibrating group of input data points is given to the NFS, node output is planned on a layer-by-layer basis, and rule resulting parameters are understood. An original network output vector x1 is accepted when the resultant parameters are obtained. The error vector (Y) is computed as ($Y=x_1-x_2$) as x_2 is the observed output, and the procedure concludes at the required epochs. Designed optimal user specifications of NFS models are shown in Table 4 (a). In the study, the number of M.F.s is endorsed one after the other to every input and output variable, and then the NFS model is organized and verified. Outcomes of the NFS model to predict the APE_{20} over gabion weir are shown in Fig. 4. and Table 5.

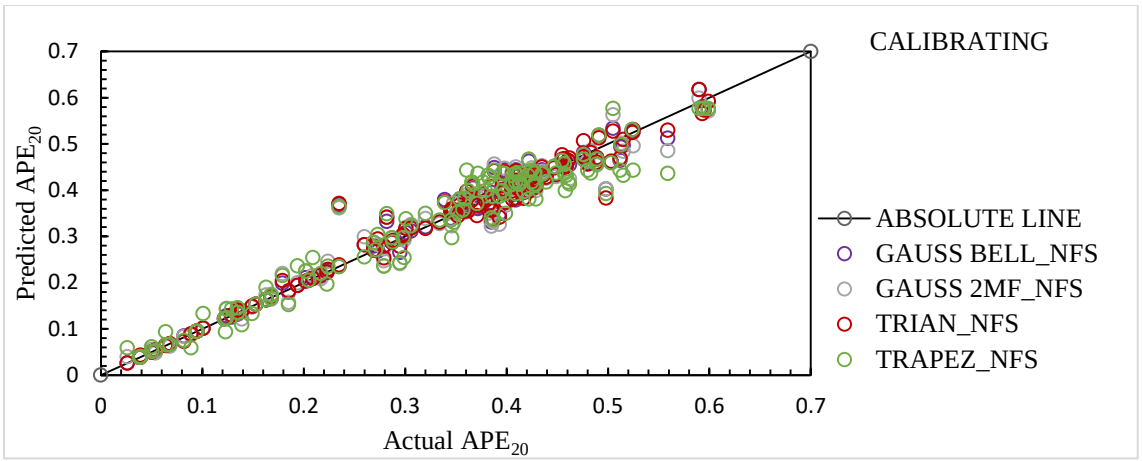

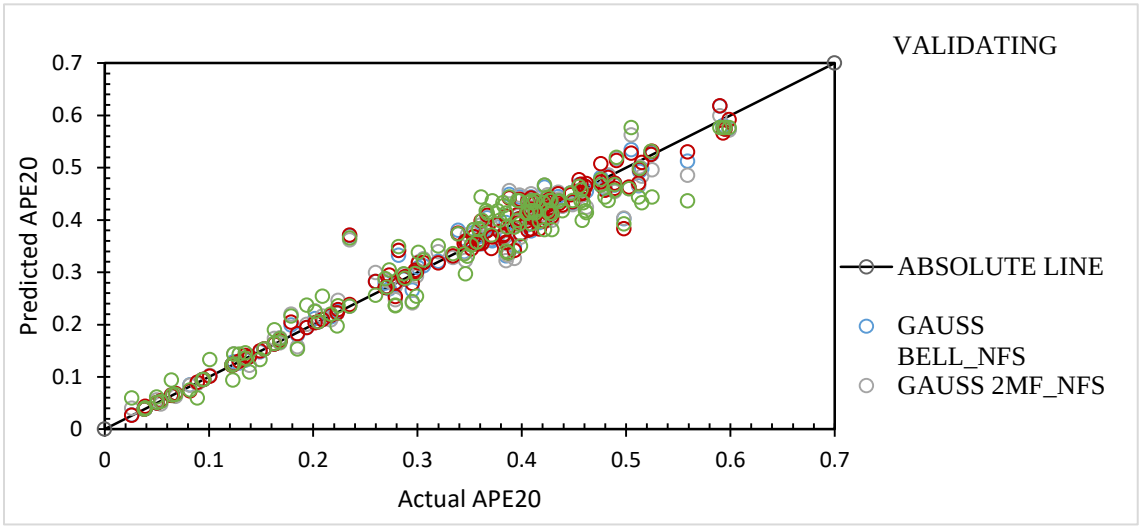

(a)

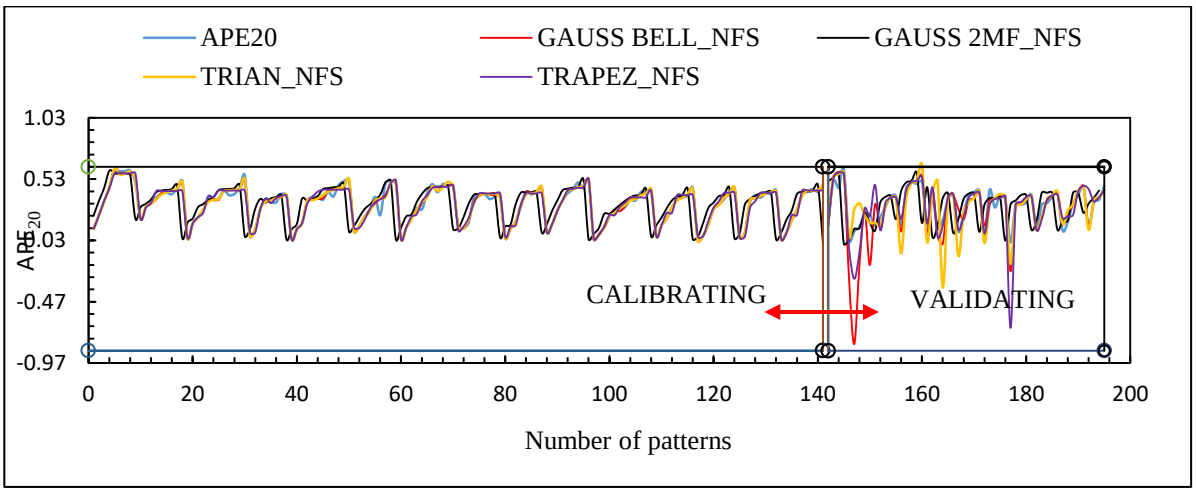

(b)

Fig. 4. (a) Performance of NFS for data pattern validation and calibration (b) Actual and predicted APE_{20} with ANFIS for calibrating and validating period.

From carefully examining Figure 4 (a), it is evident that all values predicted by proposed NFS models by and large lie near to absolute line in the case of calibration, but in the case of validation, predicted values by GAUS BELL_ NFS model are a relatively little bit away from the absolute line in comparison of other proposed NFS based models. However, the predicted values by TRAPZ _NFS model are near the absolute line. The predicted values peruse a similar case in Fig. 4 (b) by the TRAPZ _NFS model are very near to the actual values of APE_{20} both in calibrating and validating period compared to other proposed NFS-based models. This contention is further buttressed by going through Table 5. The best result is estimated by TRAPZ _NFS model as the values of R^2 =0.873 and NSE=0.852 are the highest while the error values as RMSE=0.055 and MAE=0.039 are the lowest and worse performing model GAUS BELL_NFS has been identified with the lowest value of R^2 =0. 619 and NSE=-0.034 and the highest values of RMSE=0.164 and MAE=0. 081. So, TRAPZ_NFS is performing well, but the remaining proposed NFS-based models are not performing well.

Table 5
Values of statistical performance metrics of A.I. models.

Models	Calibrating				Validating			
	R^2	NSE	RMSE	MAE	R^2	NSE	RMSE	MAE
TRIAN _NFS	0.975	0.976	0.023	0.013	0.625	0.294	0.119	0.068
TRAPZ_NFS	0.943	0.967	0.035	0.024	0.873	0.852	0.055	0.039
GAUS BELL_NFS	0.976	0.975	0.022	0.013	0. 619	-0.034	0.164	0.081
GAUS 2MF_NFS	0.966	0.943	0.027	0.017	0.626	0.084	0.136	0.069
NN	0.927	0.924	0.040	0.029	0.917	0.917	0.041	0.031
DNN	0.945	0.945	0.342	0.025	0.935	0.934	0.036	0.025

3.5. Results of NN

The NN model has been developed by using the feed-forward neural network. The feed-forward neural network has a connection between input and other layers. Since it consists of three layers of input, hidden, and output layers, it is called a multilayer perceptron. Here, the NN model is generated in three steps: data preparation for calibrating, the second requires several variations and combinations for optimum network topology, and the last is undoubtedly validating. The neurons in the hidden layers are chosen by the hit and trial process, and the best structure is one that offers values which is very close to the required targets, i.e., after estimating the error, the error is fed back to the input layer, and the process is repeated till errors become minimum. The optimum established network has five nodes in the input layer, a hidden layer with eight nodes, and an output layer having one node. Two functions in the training algorithm determine the wave signals that are processed by neurons. The training algorithm for the data set used is Polak-Ribiere conjugate gradient (trainlm) as the training function. In contrast, logsig, a transfer function, is used for the hidden layer, and tansig, the transfer function for the output layer, because this combination gives better and optimum results than other transfer functions. The NN optimal specification is enlisted in Table 4 (b). Further, the performance of the NN model has been depicted in Fig. 5(a) for calibrating and validating data points, and perusal of this figure suggests that all predicted results lie near to absolute line in both calibrating and validating. Besides this contention is further substantiated by carefully examining Fig. 5 (b). Additionally, Table 5 also suggests that the NN is performing well.

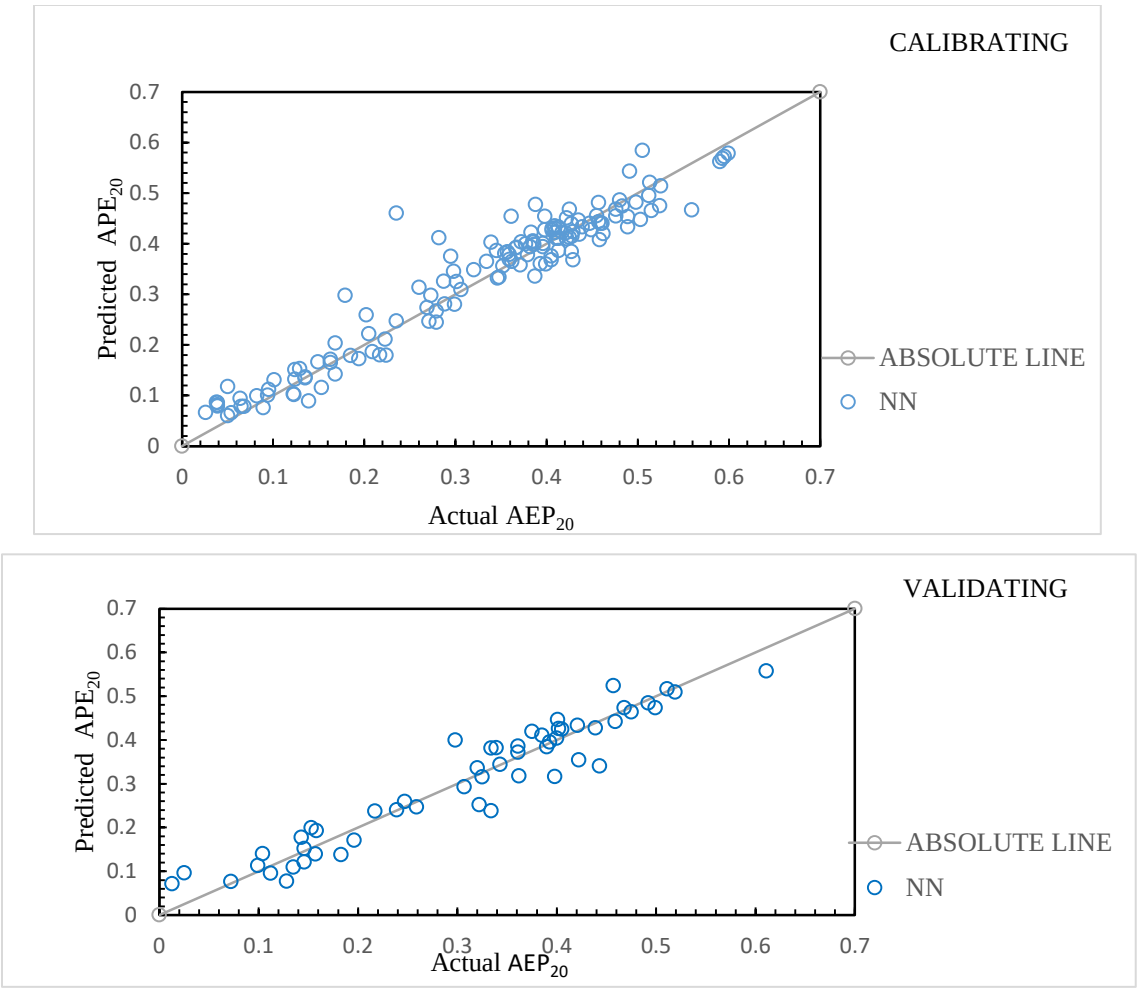

(a)

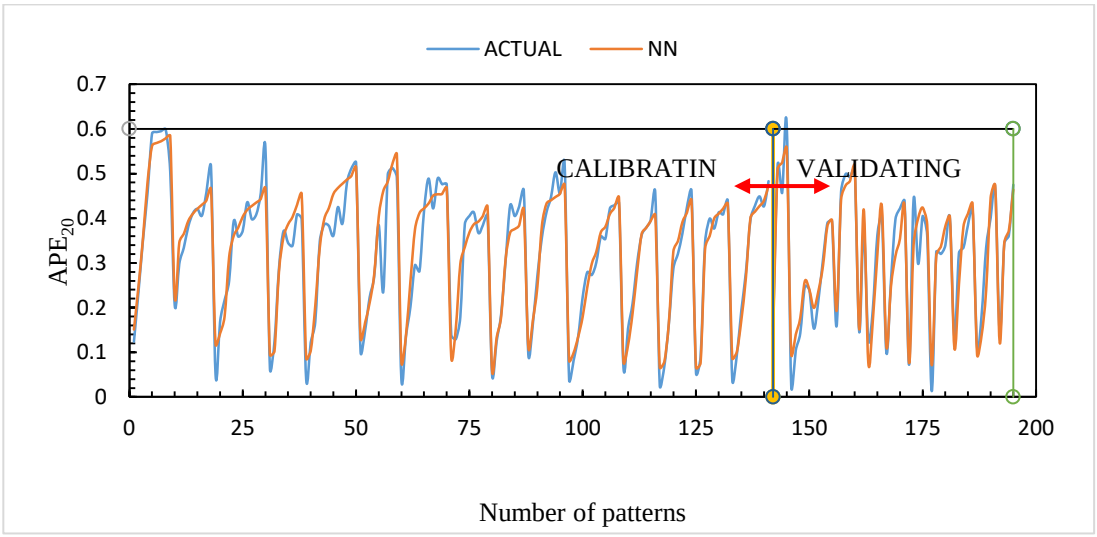

(b)

Fig. 5. (a) Performance of NN for data pattern validation and calibration, (b) APE20 measured actual and predicted using ANFIS during calibration and validation.

3.6. Results of DNN

The model is developed with different primary parameters using DNN. Among them, the optimum number of epochs have been identified for estimating the values of APE_{20} of the gabion weir with minimum error and computation cost. The optimal values of other primary parameters are found to be as values of N folds 5, fold assignment is taken as Modulo, the encoding scheme is chosen as One Hotinternal, and distribution has been found as Gaussian. While remaining optimized parameters are shown in Table 4 (c). The result variations for calibrating (training) and validating in respect of iterations (epochs) are shown in Fig. 6 (a). It is noticed that when the epochs touch 7200, the deviance acquires asymptotic to the x-axis. Hence, the values of epochs are chosen as 8241. Figs. 6 (b & c) show the scatter plot between predicted and actual APE_{20}. It could be observed that barring some predicted points either in calibrating or validating stages. All predicted points, by and large, lie near the absolute line. Besides, this aspect is further strengthened by Table 5, where statistical values of R^2 and RMSE are found to be highest and lowest, respectively, for the DNN model, demonstrating that the DNN is the best model.

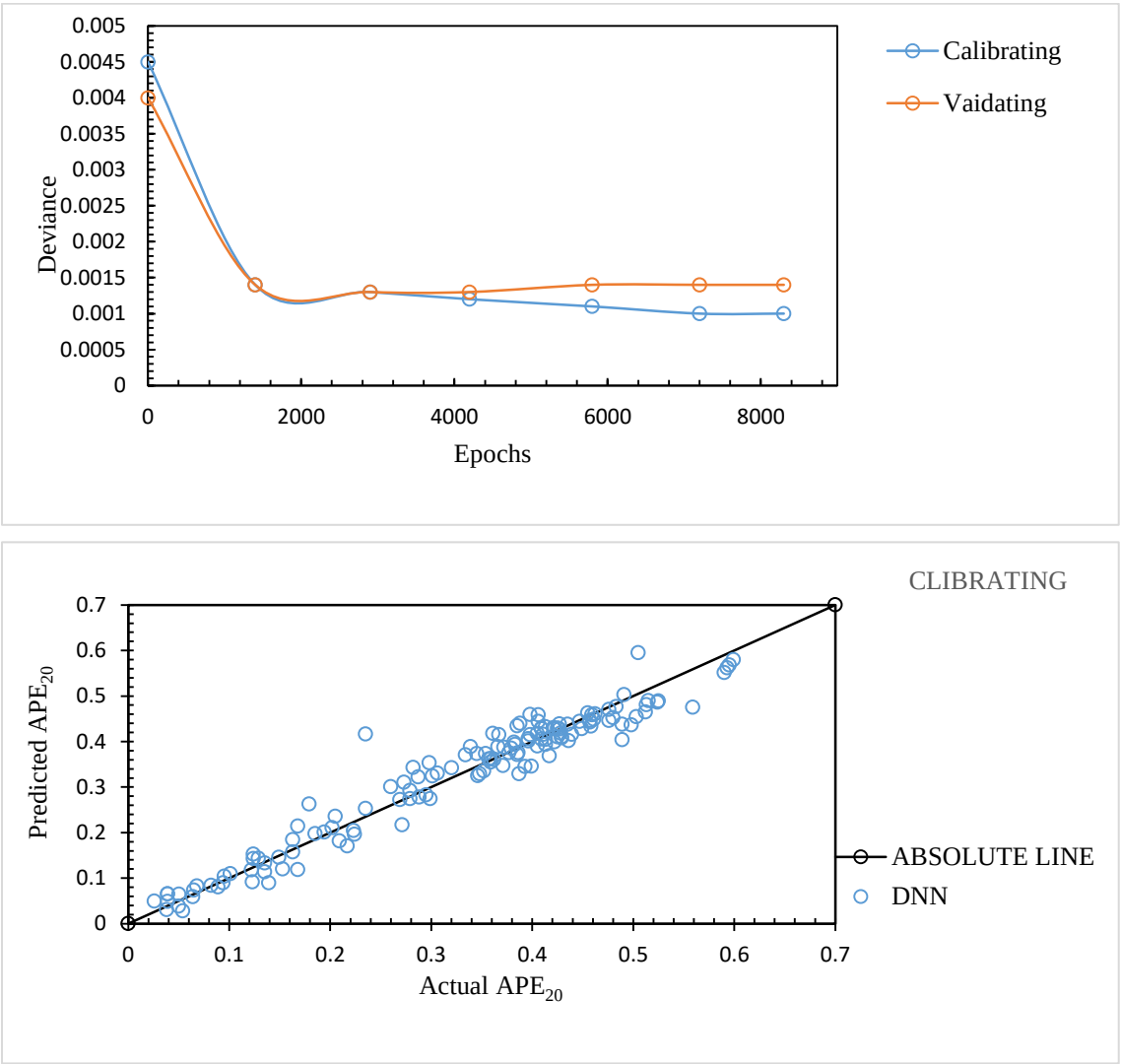

(a)

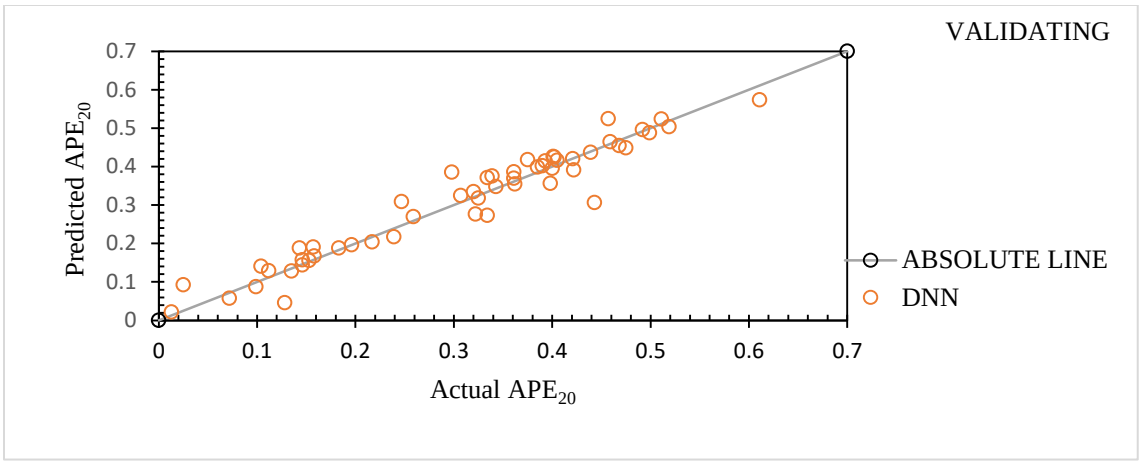

(b)

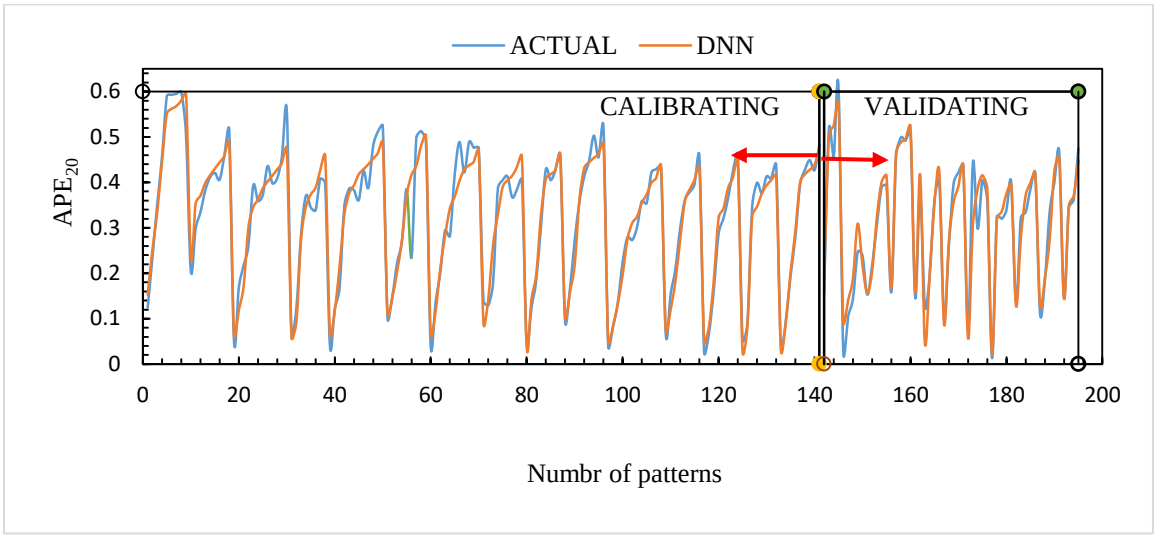

(c)

Fig. 6. (a) The deviance for calibrating and validating to epochs (b) Performance of DNN for calibrating and validating for data patterns (c) Actual and predicted APE_{20} with DNN for calibrating and validating period.

3.7. Results of MLR and mathematical models

Fig. 7 (a) for dataset ranges reported in Table 3 depicts scatter diagram comparisons of the existing mathematical relations and MLR model, which are revealed in Table 1. These plots underline the excessive scattering of the datasets along the absolute line except MLR, asserting the poor compatibility between actual values and the mathematical models' predictions. It is observed that values of calibrating and validating outcomes are lying away from the absolute line except for the MLR and, to some extent, of the Preul and Holler [27] model. Further, this contention is also strengthened by observing Table 6, where the accuracy for MLR is high, followed by Preul and Holler [27]. Other proposed mathematical models viz. Markofsky and Kobus [23], Nakasone [24], and Watson et al. [28] possess very high errors. Moreover, from the perusal of Fig. 7 (b), it is again clear that predicted values by the MLR model lie near the actual values of the APE_{20}.

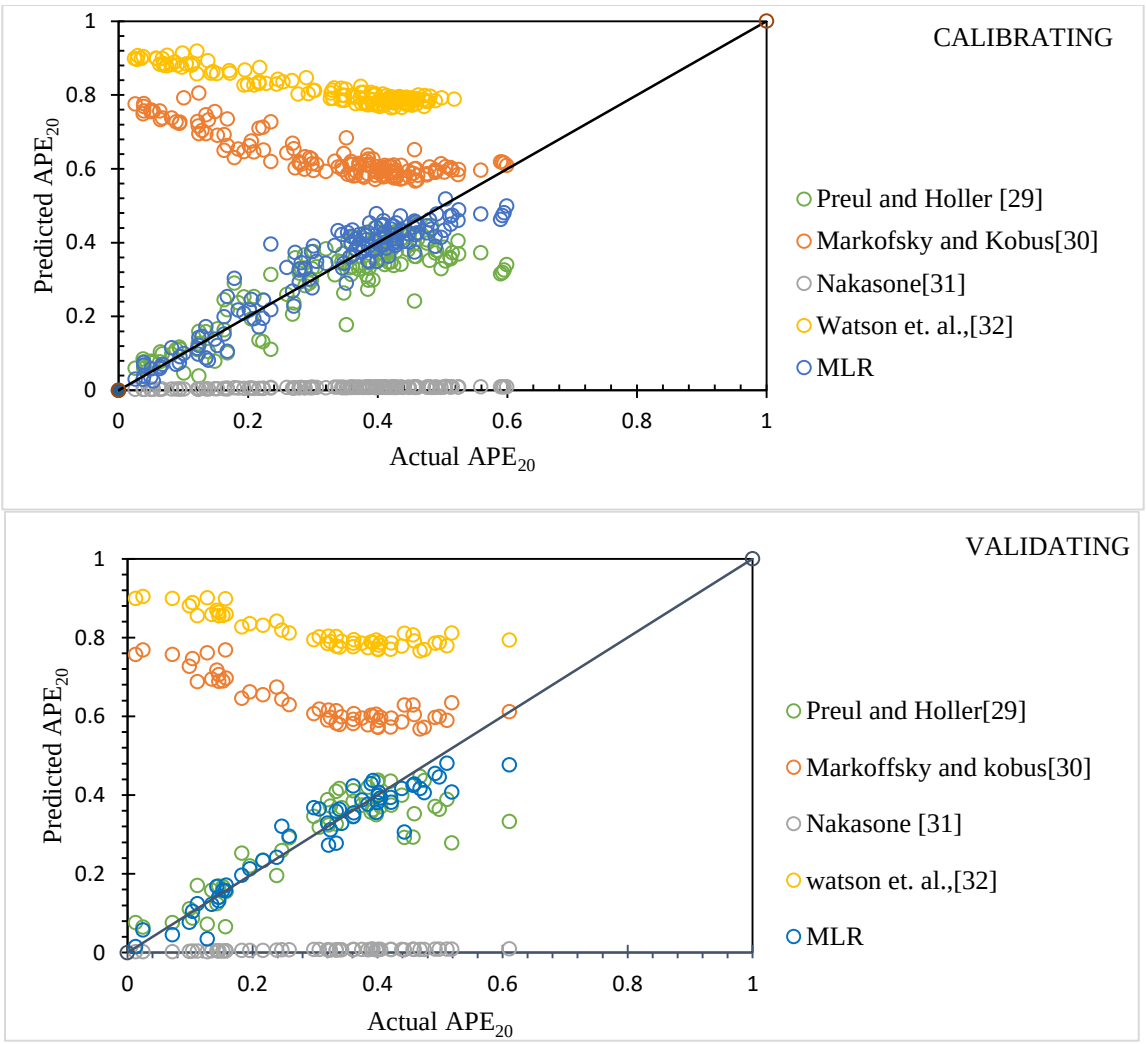

(a)

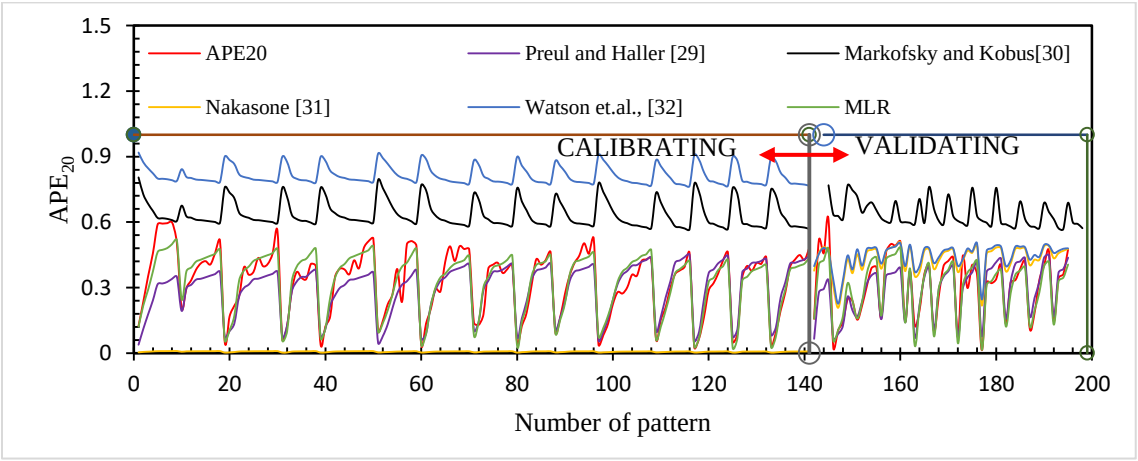

(b)

Fig. 7. (a) Performance of MLR and empirical relations for calibrating and validating for data patterns, (b) Actual and predicted APE_{20} with MLR and empirical relations for calibrating and validating period.

Table 6
Values of statistical performance metrics of conventional models.

Models	Calibrating				Validating			
	R^2	NSE	RMSE	MAE	R^2	NSE	RMSE	MAE
Naksone [1987]	0.871	-4.76	0.351	0.320	0.879	-4.51	0.334	0.303
Watson et al., [1998]	0.775	-11.63	0.519	0.486	0.762	-13.22	0.537	0.505
Markofsky and Kobus [1978]	0.740	-5.31	0.367	0.308	0.729	-6.17	0.381	0.327
Preul and Haller [1969]	0.741	0.691	0.081	0.589	0.727	0.712	0.076	0.052
MLR (present study)	0.893	0.893	0.047	0.037	0.905	0.897	0.045	0.033

3.8. Comparisons of results

The predictions of NFS, NN, DNN, and empirical models have been assessed graphically. Subsequently, statistical interpretations of its models' accuracy are examined. Fig. 8 depicts scatter plots, Taylor diagrams, etc., for comparisons of soft computing models, while Fig. 9 is that of empirical relations. Primarily, these graphs, particularly of proposed soft computing models of DNN, NN, TRAPZ_NFS, and MLR, highlight the excellent alignment of the predicted values along the absolute line of the graph (Fig. 8 a), supporting the acceptable agreement between the models' predictions and the actual values in both calibrations as well as validation stages. These arguments are further strengthened by the perusal of Tables 5 and 6, which sum up the statistical measures for the considered models where the performance of these models' estimation is assessed utilizing the statistical indices of R^2, NSE, and RMSE, MAE. It can be observed that the best-performing model DNN in validation provides high values of R^2 =0.935, NSE=0.934 and the least value of RMSE=0.036, MAE=0.025 which the NN follows with R^2 =0.917, NSE=0.917 and the value of RMSE=0.041, MAE=0.031 however, the TRAPZ _NFS with R^2 =0.873, NSE=0.852 and the value of RMSE=0.055, MAE=0.039 is third performing NFS model in soft computing model categories in in the validating stage. Besides, from the perusal of the Taylor diagram of validating (Fig. 8 b), the DNN model lies nearest to the actual value, and it is followed by the NN model. This aspect is further reinforced by observing Fig 8 c, where the DNN value is very near to the actual value, which is again followed by the NN model. Similarly, by visualizing the violin plot (Fig. 8 d), it is again clear that the size of the relative error is minimum in the case of the DNN model, and again it is followed by the NN model and other models.

Moreover, the MLR model with R^2 =0.905, NSE=0.897 and, RMSE=0.045, MAE=0.033 performs the best among classical empirical equations and even better than the NFS model (Tables 5 & 6). Furthermore, the values predicted by Markofsky and Kobus [23], Nakasone [24], and Watson et al. [28] lie beyond the $\pm$ 25 % error line (Fig. 9 a) in both calibrating and validating stages where Watson et al. [28], as well as Markofsky and Kobus [23], overestimate the APE_{20} as their predicted data points lie above the bisector line.

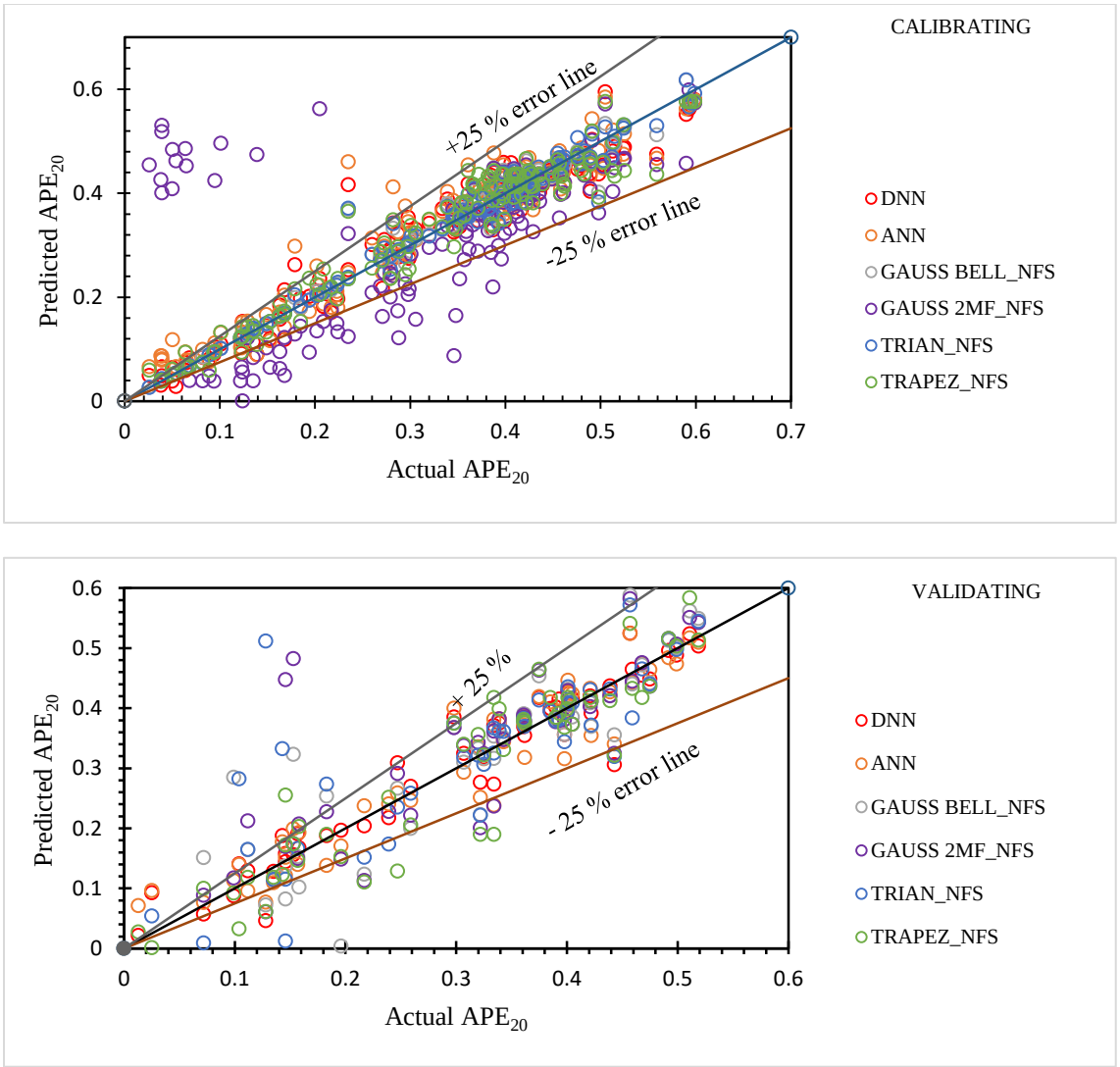

(a)

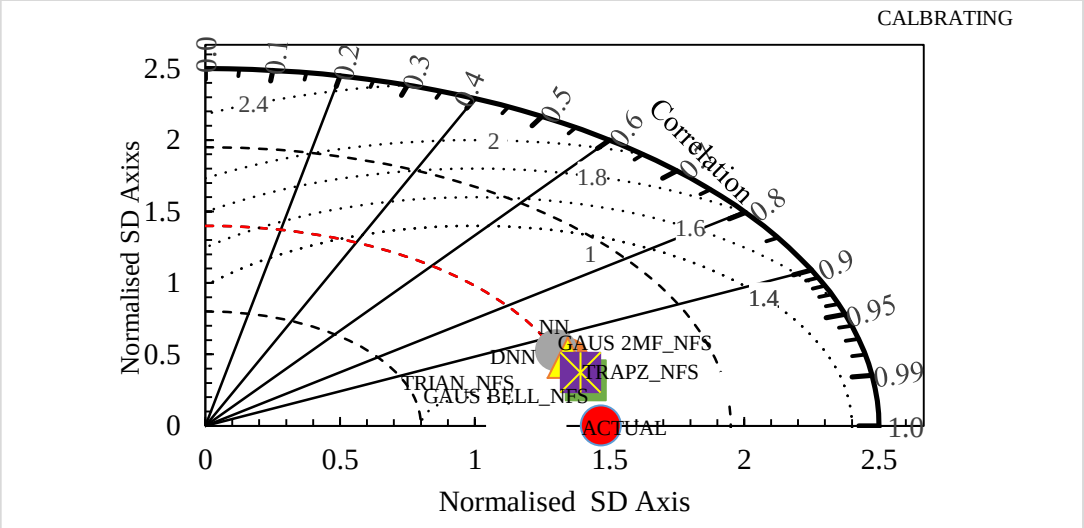
CALBRATING
Normalised SD Axixs
Normalised SD Axis
Correlation
NN
GAUS 2MF_NFS
DNN
TRAPZ_NFS
TRIAN_NFS
GAUS BELL_NFS
ACTUAL

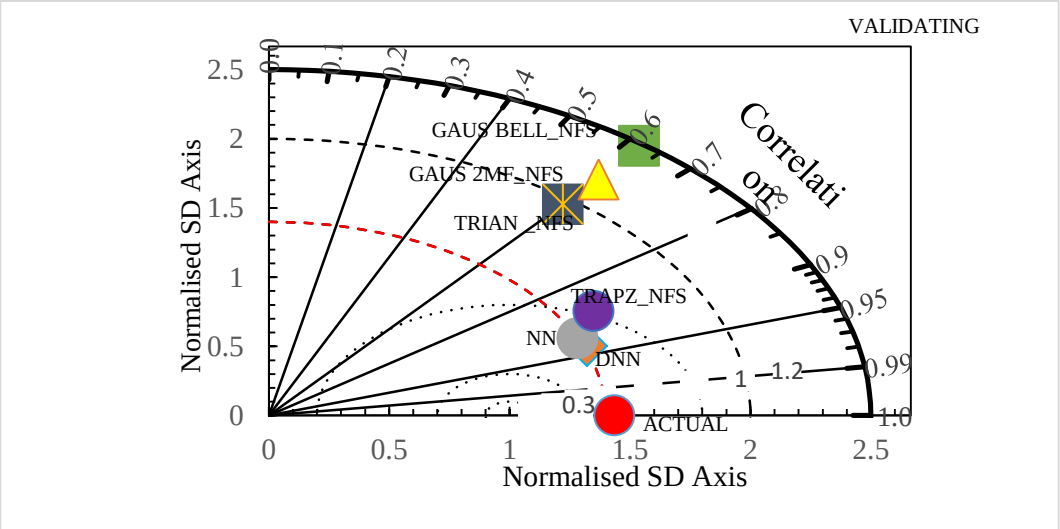
VALIDATING
Normalised SD Axis
Normalised SD Axis
Correlation
GAUS BELL_NFS
GAUS 2MF_NFS
TRIAN _NFS
TRAPZ_NFS
NN
DNN
ACTUAL

(b)

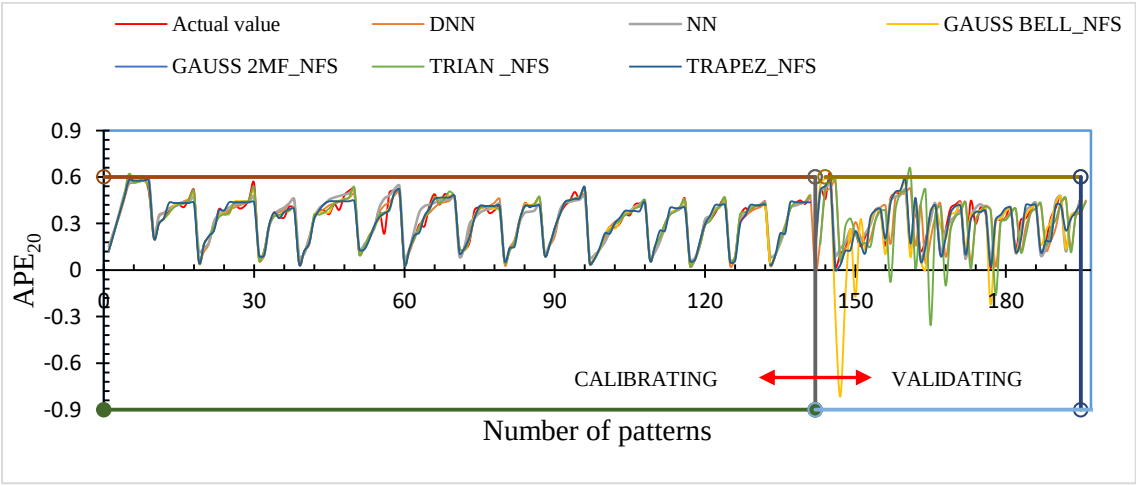
Actual value
DNN
NN
GAUSS BELL_NFS
GAUSS 2MF_NFS
TRIAN _NFS
TRAPEZ_NFS
APE20
Number of patterns
CALIBRATING
VALIDATING

(c)

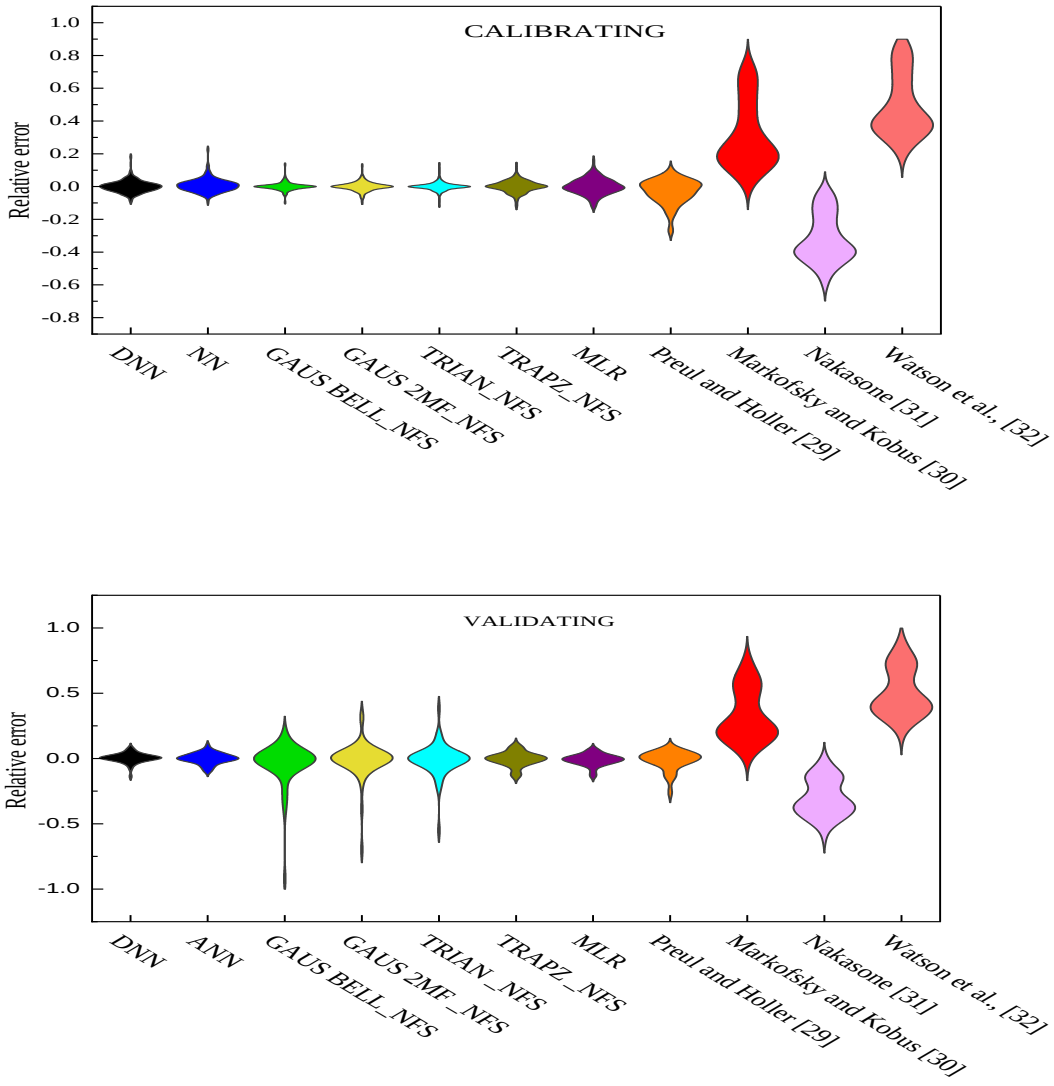

(d)

Fig. 8. (a) Performance of proposed AI models for calibrating and validating for data patterns, (b) Normalized Taylor diagram displaying the performances of evaluated proposed AI models, (c) Actual and predicted APE_{20} with AI-models for calibrating and validating period (d) Violin error plots for all models.

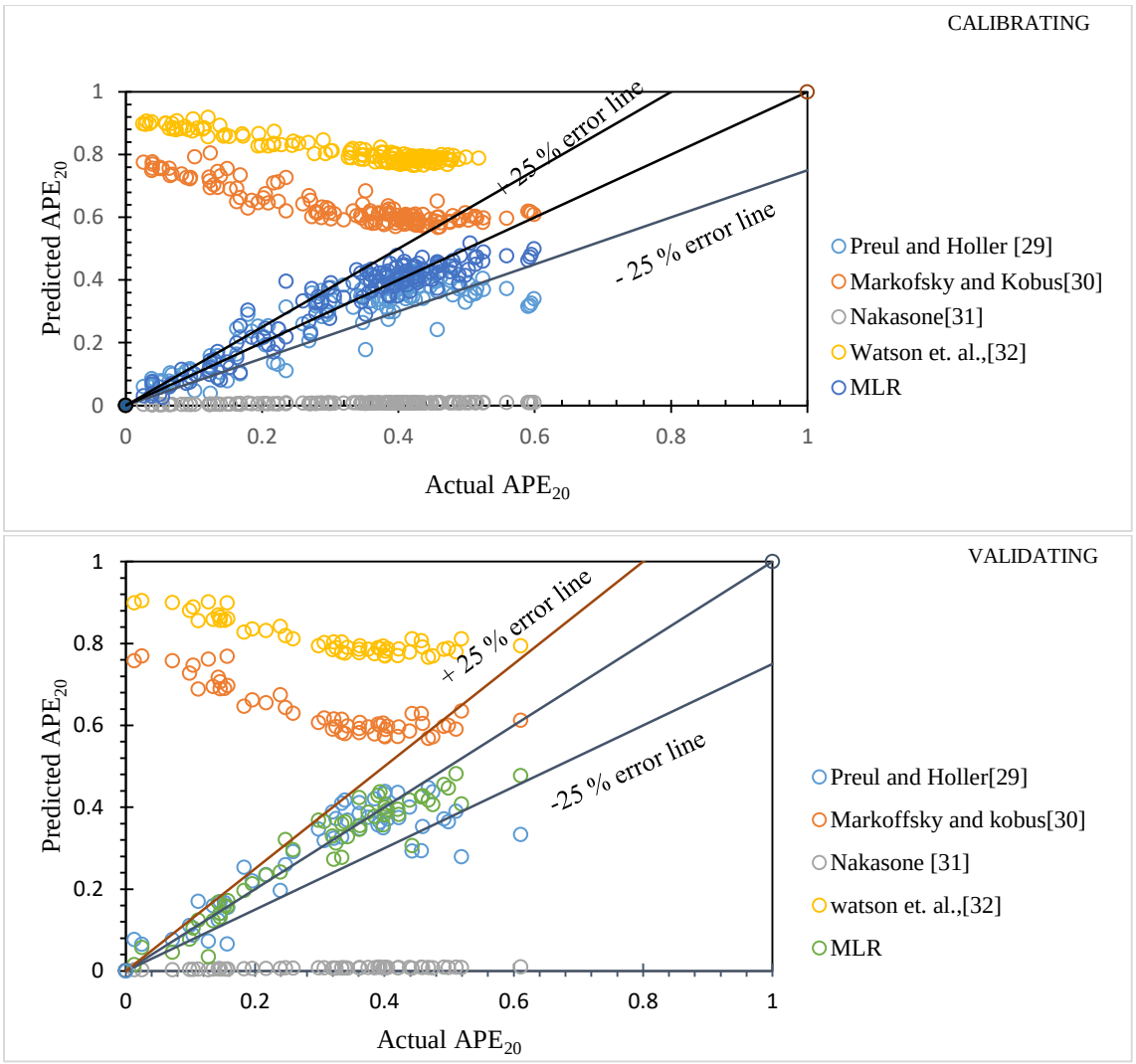
CALIBRATING
Predicted APE20
Actual APE20
+ 25 % error line
- 25 % error line
Preul and Holler [29]
Markofsky and Kobus[30]
Nakasone[31]
Watson et. al.,[32]
MLR
VALIDATING
Predicted APE20
Actual APE20
+ 25 % error line
-25 % error line
Preul and Holler[29]
Markoffsky and kobus[30]
Nakasone [31]
watson et. al.,[32]
MLR

(a)

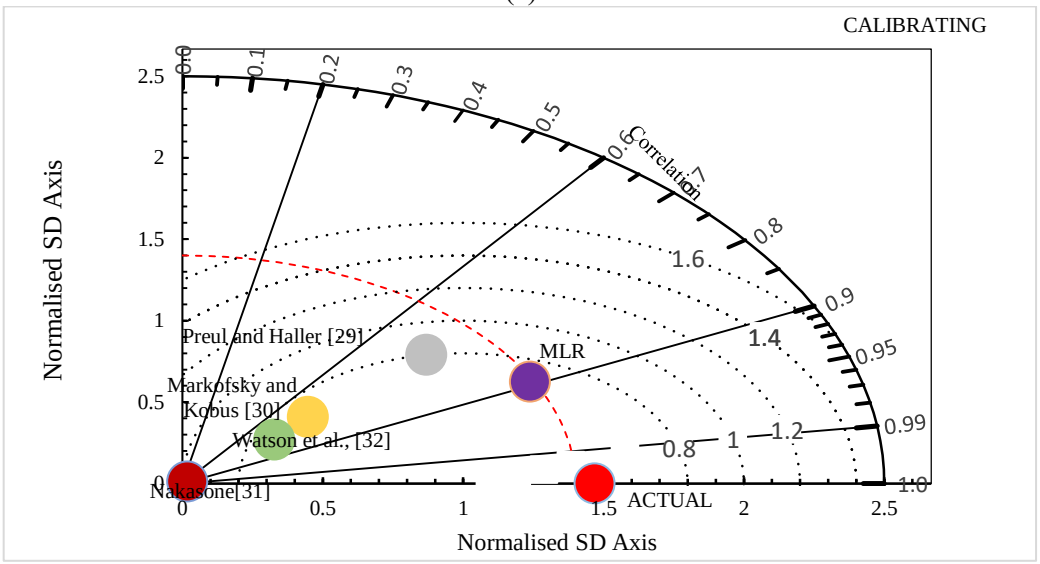
CALIBRATING
Normalised SD Axis
Correlation
Preul and Haller [29]
Markofsky and Kobus [30]
Watson et al., [32]
Nakasone[31]
MLR
ACTUAL
Normalised SD Axis

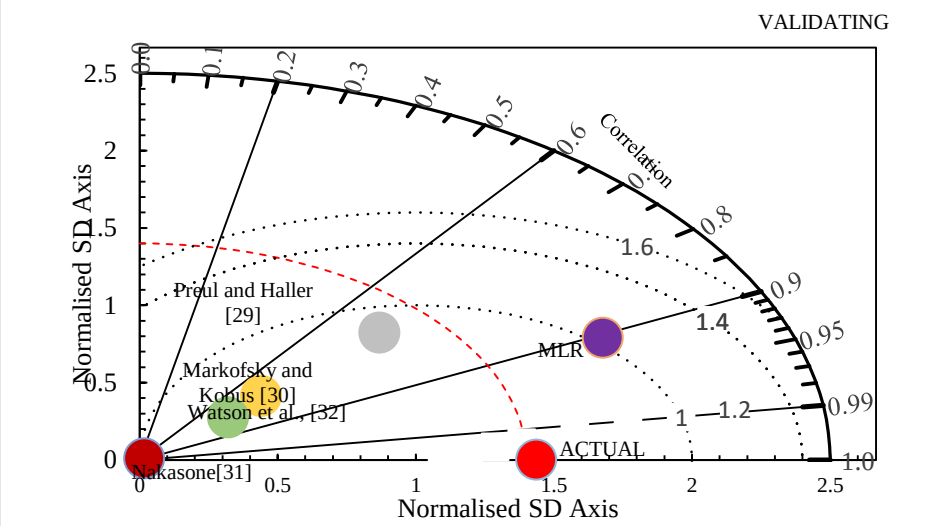

(b)

Fig. 9. (a) Performance of MLR and empirical relations for calibrating and validating for data patterns (b) Taylor diagram showing the performances of evaluated MLR and empirical relations.

However, Nakasone [24] appears to be underestimating the APE_{20} of the gabion weir as its predicted data points lie below the bisector line, but Preul and Holler [27] performance, as well as its predicted values, lie within ± 25 % error line in both stages of calibrating and validating.

Fig. 9 b also suggests the same results as MLR is very near to the actual value, followed by Preul and Holler [27]. Similarly, by visualizing the Violin error plots of Fig 8 d, the size of relative error for MLR is the least, followed by Preul and Holler [27], which suggests that the MLR model is the best among the empirical relations.

Comparatively poor performance of empirical models compared to the proposed soft computing-based models is attributed because these models do not have enough potential to tackle all dimensions, which are responsible for a nonlinear and complex phenomenon that occurs during the aeration process at broad crested gabion weir, in contrast, the soft computing models use machine learning algorithms that do not require any limiting assumptions on the form of the model further the fact is that they can generalize, track and detect complex nonlinear relationships between independent and dependent parameters.

3.9. Importance of input variables and sensitive study

The selection of the independent influencing parameters is paramount for the generation of illustrative models as the predictive potential of the generated models mainly depends on the choice of input parameters George, [44]. The determination of input variables arises when

investigators pursue a predictive method that validates satisfaction or redundancy among the input parameters, which leads to multiple recti-linearity [45]. However, recti-linearity occurs when a single predictor parameter can be estimated with considerable accuracy in numerous regression equations. If there are more than two predictor parameters, then there would be an appreciable loss in statistical importance of the model, which is called multiple recti-linearity. Different from recti-linearity, multiple recti-linearity might not be feasible to forecast before perceiving its impact on the model as part of the predictor parameters might have a low association level. A multiple recti-linearity does not lessen the predictive potential or consistency of the model in totality, at minimum, in the datasets; it merely surges the intricacy of the model and influences computations about distinctive predictors. Thus, an easy model equation nevertheless comprises valuable material that is constantly desirable. Having selected the critical variables, a sensitive study determines the relative significance of the input variable on the $APE_{20.}$ The analysis is performed by removing one input parameter and appraising the impact of that very parameter on the prediction of the $APE_{20.}$ The sensitivity study of the input is presented in Fig.10 using the best-performing DNN model. The most influencing input variable has been found as discharge per unit width (q), which has the most significant impact on the APE_{20} of the gabion weir, which is followed by drop height (H_o); however, porosity(n) and height of weir (P) both are equally third important variables. The least important variable is the mean size (d_{50}) of gabion particles which has the most negligible impact on the APE_{20}

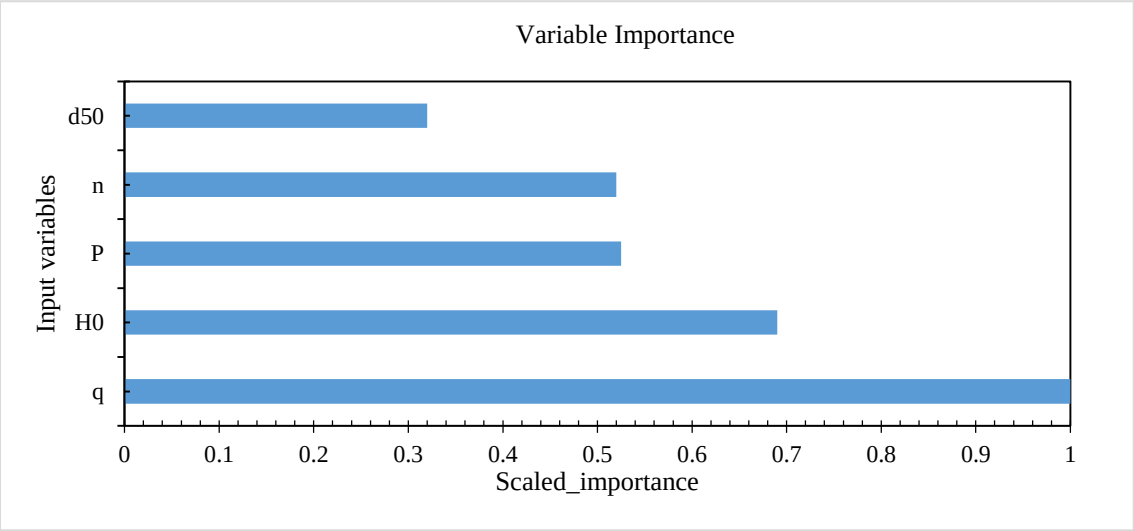

Fig. 10. Sensitivity study for the relative importance of input parameters.

4. Conclusions and suggestions

Gabion weir is an alternative economical and effective hydraulic device for conventional weir, mainly when the head of water is low to moderate. The dissolved oxygen intensity is one of the crucial determinants in evaluating hydrosphere health. This work is one of the efficient studies utilizing NN, NFS, DNN, and MLR to generate models for predicting gabion weir aeration performance efficiency. Laboratory tests are carried out for datasets to calibrate and validate the proposed models. The DNN with the highest values of R^2 =0. 935, NSE=0.934, and the lowest values of RMSE =0.036, MAE=0.025 outperforms all the proposed models besides, predicted values by this model lie very near along the agreement diagram further, the model also lies very near to the actual value in the Taylor diagram along with relative error size in violin plot is minimum which is followed by the NN model having R^2 =0.917, NSE=0.917 and RMSE =0.041, MAE=0.031 which is giving comparable results in validating stage. The third best-performing model amongst proposed AI models is TRAPZ _NFS with R^2 =0.873, NSE=0.852, and the value of RMSE=0.055, MAE=0.039. But other remaining proposed NFS-based models could not perform better with the low value of correlations and high values of errors for an unknown validating dataset. Further, it has also been found that the mathematical model generated by MLR is performing better than the other proposed mathematical models for this dataset range. Additionally, the sensitivity study suggests that discharge per unit width (q) has the highest significant impact on the output results of the APE_{20} for the gabion weir, followed by drop height (H_o). Nevertheless, it has been recognized that the dataset is comparatively smaller in size and extent. So, future works should incorporate a bigger volume and broader range of datasets to allow the models to be more versatile and generalize on the gabion weir aeration performance efficiency.

Funding

This research received no external funding.

Conflicts of interest

The authors declare no conflict of interest.

Authors contribution statement

NKT, K.L.: Conceptualization; NKT, K.L.: Data curation; NKT, K.L.: Formal analysis; NKT, K.L.: Investigation; NKT, K.L., S.R.: Methodology; K.L.: Project administration; K.L.: Resources; NKT: Software; S.R., NKT: Supervision; NKT, S.R.: Validation; NKT, K.L., S.R.:

Visualization; NKT, K.L.: Roles/Writing – original draft; NKT, K.L., S.R.: Writing – review & editing.

References

[1] Chu K, Hua Z, Ji L. AERATION AT OVERFLOW DAMS WITH CURVED SURFACES BY DIFFERENT FLASHBOARD SPILLWAYS. J Environ Eng Landsc Manag 2014;22:226–36. https://doi.org/10.3846/16486897.2014.901226.

[2] Resit G, Ozgur K, O. FD, M. EE. Applicability of Several Soft Computing Approaches in Modeling Oxygen Transfer Efficiency at Baffled Chutes. J Irrig Drain Eng 2017;143:4016085. https://doi.org/10.1061/(ASCE)IR.1943-4774.0001153.

[3] Michael P, Jill L, H. HW. Chute Aerators: Preaerated Approach Flow. J Hydraul Eng 2011;137:1452–61. https://doi.org/10.1061/(ASCE)HY.1943-7900.0000417.

[4] L. UA, S. GJ, W. JD. Modeling Total Dissolved Gas Concentration Downstream of Spillways. J Hydraul Eng 2008;134:550–61. https://doi.org/10.1061/(ASCE)0733-9429(2008)134:5(550).

[5] Alp E, Melching CS. Allocation of supplementary aeration stations in the Chicago waterway system for dissolved oxygen improvement. J Environ Manage 2011;92:1577–83. https://doi.org/10.1016/j.jenvman.2011.01.014.

[6] Khdhiri H, Potier O, Leclerc J-P. Aeration efficiency over stepped cascades: Better predictions from flow regimes. Water Res 2014;55:194–202. https://doi.org/10.1016/j.watres.2014.02.022.

[7] Davide W, Hubert C. Hydraulics, Air Entrainment, and Energy Dissipation on a Gabion Stepped Weir. J Hydraul Eng 2014;140:4014046. https://doi.org/10.1061/(ASCE)HY.1943-7900.0000919.

[8] Kaya N, Emiroglu ME. Study of oxygen transfer efficiency at baffled chutes. Proc Inst Civ Eng - Water Manag 2010;163:447–56. https://doi.org/10.1680/wama.900029.

[9] Dursun OF, Talu MF, Kaya N, Alcin OF. Length prediction of non-aerated region flow at baffled chutes using intelligent nonlinear regression methods. Environ Earth Sci 2016;75:680. https://doi.org/10.1007/s12665-016-5486-8.

[10] Tiwari NK. Evaluating hydraulic jump oxygen aeration by experimental observations and data driven techniques. ISH J Hydraul Eng 2021;27:601–15. https://doi.org/10.1080/09715010.2019.1658551.

[11] Kumar M, Tiwari NK, Ranjan S. Experimental Study on Oxygen Mass Transfer Characteristics by Plunging Hollow Jets. Arab J Sci Eng 2021;46:4521–32. https://doi.org/10.1007/s13369-020-04975-9.

[12] Tiwari NK, Sihag P. Prediction of oxygen transfer at modified Parshall flumes using regression models. ISH J Hydraul Eng 2020;26:209–20. https://doi.org/10.1080/09715010.2018.1473058.

[13] Dursun OF. An experimental investigation of the aeration performance of parshall flume and venturi flumes. KSCE J Civ Eng 2016;20:943–50. https://doi.org/10.1007/s12205-015-0645-0.

[14] Baylar A, Hanbay D, Batan M. Application of least square support vector machines in the prediction of aeration performance of plunging overfall jets from weirs. Expert Syst Appl 2009;36:8368–74. https://doi.org/10.1016/j.eswa.2008.10.061.

[15] Baylar A, Unsal M, Ozkan F. GEP modeling of oxygen transfer efficiency prediction in aeration cascades. KSCE J Civ Eng 2011;15:799–804. https://doi.org/10.1007/s12205-011-1282-x.

[16] Kumar M, Tiwari NK, Ranjan S. Soft computing based predictive modelling of oxygen transfer performance of plunging hollow jets. ISH J Hydraul Eng 2022;28:223–33. https://doi.org/10.1080/09715010.2020.1752831.

[17] Kumar M, Tiwari NK, Ranjan S. Kernel function based regression approaches for estimating the oxygen transfer performance of plunging hollow jet aerator. J Achiev Mater Manuf Eng 2019;95. https://doi.org/10.5604/01.3001.0013.7917.

[18] Kumar M, Ranjan S, Tiwari NK. Oxygen transfer study and modeling of plunging hollow jets. Appl Water Sci 2018;8:121. https://doi.org/10.1007/s13201-018-0740-8.

[19] Bodana D, Tiwari NM, Ranjan S, Ghanekar U. Estimation of the depth of penetration in a plunging hollow jet using artificial intelligence techniques. Arch Mater Sci Eng 2020;103. https://doi.org/10.5604/01.3001.0014.3354.

[20] Sattar AA, Elhakeem M, Rezaie-Balf M, Gharabaghi B, Bonakdari H. Artificial intelligence models for prediction of the aeration efficiency of the stepped weir. Flow Meas Instrum 2019;65:78–89. https://doi.org/https://doi.org/10.1016/j.flowmeasinst.2018.11.017.

[21] Sharafati A, Haghbin M, Tiwari NK, Bhagat SK, Al-Ansari N, Chau K-W, et al. Performance evaluation of sediment ejector efficiency using hybrid neuro-fuzzy models. Eng Appl Comput Fluid Mech 2021;15:627–43. https://doi.org/10.1080/19942060.2021.1893224.

[22] Gameson ALH. Weirs and the aeration of rivers. J Inst Wat Engrs 1957;11:477–90.

[23] Mark M, Helmut K. Unified Presentation of Weir-Aeration Data. J Hydraul Div 1978;104:562–8. https://doi.org/10.1061/JYCEAJ.0004980.

[24] Hideo N. Study of Aeration at Weirs and Cascades. J Environ Eng 1987;113:64–81. https://doi.org/10.1061/(ASCE)0733-9372(1987)113:1(64).

[25] T. AS, Pavel N. Oxygen Transfer at Hydraulic Structures. J Hydraul Div 1978;104:1521–40. https://doi.org/10.1061/JYCEAJ.0005100.

[26] Tsang C. Hydraulic and aeration performance of labyrinth weirs. 1987.

[27] Preul HC, Holler AG. Reaeration through low dams in the Ohio River. Proc. 24th Ind. waste Conf. two, Purdue Univ. Lafayette, Indiana, 1969.

[28] Watson CC, Walters RW, Hogan SA. Aeration performance of low drop weirs. J Hydraul Eng 1998;124:65–71. https://doi.org/10.1061/(ASCE)0733-9429(1998)124:1(65).

[29] Luxmi KM, Tiwari NK, Ranjan S. Application of soft computing approaches to predict gabion weir oxygen aeration efficiency. ISH J Hydraul Eng 2022:1–15. https://doi.org/10.1080/09715010.2022.2050311.

[30] Luxmi KM, Tiwari A, Tiwari NK, Vajesnayee SR. Development and Evaluation of Soft Computing Models for Montana Flume Aeration BT - Advances in Chemical, Bio and Environmental Engineering. In: Ratan JK, Sahu D, Pandhare NN, Bhavanam A, editors., Cham: Springer International Publishing; 2022, p. 167–80.

[31] Tiwari A, Ojha CSP, Tiwari NK, Ranjan S. Montana Flume Aeration Performance Evaluation with Machine Learning Models. J Inst Eng Ser A 2023;104:175–86. https://doi.org/10.1007/s40030-022-00706-5.

[32] Aufmann R, Vernon B. College Trigonometry. Cengage Learn 2007.

[33] Srinivas R, Tiwari NK. Oxygen aeration efficiency of gabion spillway by soft computing models. Water Qual Res J 2022;57:215–32. https://doi.org/10.2166/wqrj.2022.009.

[34] Munish K, Tiwari NK, Subodh R. Application of Machine Learning Methods in Estimating the Oxygenation Performance of Various Configurations of Plunging Hollow Jet Aerators. J Environ Eng 2022;148:4022070. https://doi.org/10.1061/(ASCE)EE.1943-7870.0002068.

[35] Srinivas R, Tiwari NK. Modeling of the oxygen aeration performance efficiency of gabion spillways. Water Pract Technol 2022;17:2317–33. https://doi.org/10.2166/wpt.2022.139.

[36] Tiwari NK, Luxmi KM, Ranjan S. Estimating gabion weir oxygen transfer with data mining. Water Qual Res J 2022;58:22–40. https://doi.org/10.2166/wqrj.2022.023.

[37] Singh A, Singh B, Sihag P. Experimental Investigation and Modeling of Aeration Efficiency at Labyrinth Weirs. J Soft Comput Civ Eng 2021;5:15–31. https://doi.org/10.22115/scce.2021.284637.1311.

[38] Ghanizadeh AR, Delaram A, Fakharian P, Armaghani DJ. Developing Predictive Models of Collapse Settlement and Coefficient of Stress Release of Sandy-Gravel Soil via Evolutionary Polynomial Regression. Appl Sci 2022;12:9986. https://doi.org/10.3390/app12199986.

[39] Rezazadeh Eidgahee D, Jahangir H, Solatifar N, Fakharian P, Rezaeemanesh M. Data-driven estimation models of asphalt mixtures dynamic modulus using ANN, GP and combinatorial GMDH approaches. Neural Comput Appl 2022;34:17289–314. https://doi.org/10.1007/s00521-022-07382-3.

[40] Jang J-SR. ANFIS: adaptive-network-based fuzzy inference system. IEEE Trans Syst Man Cybern 1993;23:665–85. https://doi.org/10.1109/21.256541.

[41] Goodfellow I, Bengio Y, Courville A. Deep learning. MIT press; 2016.

[42] Nair V, Hinton GE. Rectified linear units improve restricted boltzmann machines. Proc. 27th Int. Conf. Mach. Learn., 2010, p. 807–14. https://doi.org/10.1007/s00521-022-07382-3.

[43] Srivastava N, Hinton G, Krizhevsky A, Sutskever I, Salakhutdinov R. Dropout: a simple way to prevent neural networks from overfitting. J Mach Learn Res 2014;15:1929–58.

[44] George EI. The Variable Selection Problem. J Am Stat Assoc 2000;95:1304–8. https://doi.org/10.1080/01621459.2000.10474336.

[45] Fox J. Regression diagnostics: An introduction. Sage publications; 2019, ISBN: 978-1-5443-7522-9.